EXECUTIVE SUMMARY

This document details the proposal for the **Co**herent **D**iffraction **I**maging beamline (CoD**I**) at ALBA **II**. The main scope and uniqueness of CoD**I** is to perform *in situ* and *operando* characterization of thick samples with nanometer resolution exploiting:

(i) the coherence of ALBA **II**;
(ii) the possibility of building a 250 meters long beamline;
(iii) the availability of room for a unique sample detector distance of 20 m, as a new building will be constructed.

To achieve these goals, CoD**I** is optimized for:

(i) A range of energies between 10-30 keV to probe thick samples in their relevant conditions,
(ii) An efficient control of the coherence and flux using a secondary source to tailor the beam features of the experiments to be carried out,
(iii) The use of a nano-focusing Kirkpatrick–Baez (KB) mirror (sub-50 nm focus) that enable a long working distance, more than 150 mm, that allows to accommodate *in situ* and *operando* sample environments,
(iv) Multilayer Laue lenses (MLLs) to produce the ultimate efficient nano-focus (sub-10 nm focus) for ultra-high resolution X-ray imaging,
(v) A long sample to detector distance that enables high-solid angle resolution with current direct-conversion detectors.

These features will make CoD**I** not only one of the forefront beamlines for scanning nanoimaging techniques (X-ray diffraction or X-ray fluorescence) but also for coherent imaging in the forward direction (ptychography and holography) and in diffraction conditions (Bragg-CDI, Bragg-ptychography, and tele-ptychography)

As a result of its capabilities and flexibility, CoD**I** will contribute to key strategic sectors of ALBA research, the European Union, such as clean and affordable energy, health, sustainability, novel material and technology production. This is illustrated by selecting several key scientific cases that will enormously benefit from CoD**I** unique performances. With the use of scanning and coherent X-ray techniques CoD**I** will help in the better comprehension and design of catalytic reactors, semiconductors chips or nanomaterials for biology. But also, CoD**I** will help in the understanding of exoplanetary materials or geological natural process.

Finally, it is important to highlight that CoD**I** synergizes with ALBA and its current set of facilities by providing new nano-characterization capabilities for *in situ* and *operando* systems that complement:

i) The imaging capabilities of FaXToR and MISTRAL photon beamlines,
ii) The JEMCA (Joint Electron Microscopy Center at ALBA) electron microscopy platform,
iii) The InCAEM (In situ Correlative facility for Advanced Energy Materials) set of equipment.

1 - Scientific case (approximately 15 pages)

We propose CoDI to be a **Co**herent **D**iffraction **I**maging beamline at ALBA II. This experimental station will be intended to investigate materials in strategic sectors for the European Union (biotechnology and agri-food; energy transition and decarbonization; active and healthy aging; circular economy and sustainable raw materials), which complement ALBA strategic research lines.

CoDI will have as primary mission the study of *in situ* and *operando* processes with nano-focus X-rays beams in thick samples (< 500 μm), covering a large number of nanostructured materials for different technological areas (e.g. nanocatalysts, nanocrystals, nanoparticles or bio-technology). For the study of these types of thick samples a main energy range of 10-30 keV has been chosen to increase the penetration depth through the materials. Along this energy range sub-50 nm X-ray beams will be used for the study of nanostructured materials. At these energies only a long beamline with a secondary source can provide the high coherence X-ray needed for high resolution focus and the implementation of coherent X-ray diffraction imaging (CXDI) techniques as the ones desired at CoDI. We want the X-ray beam transport from CoDI to be capable of delivering the high coherent properties of the X-rays from ALBA II. The percentage of coherent photons will be maximized with a pre-focusing scheme based on focusing mirrors and a secondary source located around 50 m from the source. The main focusing technique will be a set of Kirkpatrick–Baez (KB) mirrors located 230 m from the X-ray source that will provide a focused spot down to $32x32nm^2$ at the energy of 20 keV with a working distance of 150 mm. This will allow the installation of relatively big cells to perform *in situ* and *operando* experiments in nanometer size systems such as nanoparticles (NPs) and other nanostructures materials. The expected flux in the focused beam will range from 2e11 photons/s for a high degree of coherence to 10^{12} ph/s with the full flux, at a 0.1% bandwidth at 20 keV. A second focusing method foreseen at CoDI will be a set of two multi Laue lenses (MLLs), one vertical and one horizontal, to focus the beam to $6x6nm^2$ (FWHM) with only 20% less flux compared to the KB mirror. With these properties CoDI will provide additionally several diffraction based nano-focusing techniques, as well as fluorescence mapping of functional thin films and materials. A long sample detector distance (20 m) along the forward direction will allow the use of efficient single photon counting detectors while ensuring sufficient spatial resolution for direct imaging without exceeding count rate limitations.

With X-ray beam parameters CoDI will be suitable for nano-scanning diffraction and fluorescence studies [1,2]. We propone to implement at CoDI several coherent based imaging techniques both in forward and diffraction directions, with the main focus in tomography-based imaging and Bragg coherent diffraction imaging (Bragg-CDI) [3,4]. The setup will be compatible with imaging approaches such as holotomography, ptychography [5,6], Bragg-ptychography [7] and tele-ptychography[8-10]. Tele-ptychography is a new variant of ptychography that uses an analyzer to reconstruct complex wavefronts (amplitude and phase) after the sample. his simplifies *in situ* and *operando* experiments, as the sample does not need to be scanned during the data collection. Tele-ptychography will allow to perform high resolution images of processes in complex environments both in the forward and in the diffraction directions. For this technique the sample does not need to be on the focus of the lenses as the reconstructions give the complex wave front along the propagation direction of the X-rays. A tailored setup for tele-ptychography will make CoDI at ALBA II a unique instrument in the world to study *in situ* and *operando* processes.

Phase modulation techniques exploiting the nano-focusing capabilities of CoDI will be available. These methods will allow the control of the incoming beam wavefront, and hence, the distribution of the intensity at the focal plane. Thereby, we will improve the spatial resolution and optimize the measurement efficiency favoring the *in situ* and *operando* experiments [11].

We expect to start the operation of CoDI with nano X-ray fluorescence (XRF) and nano-diffraction (XRD) and subsequently add the different techniques mentioned above in order of complexity. Our proposed strategy would be to start by 2D ptychography, holography and tele-ptychography for study semiconductors chips and open the doors of the *in situ* catalysis with the implementation of Bragg-Coherent Diffraction Imaging (Bragg-CDI). Afterwards, we will add 3D tomographic-imaging propagation phase techniques and at last Bragg-ptychography and tele-ptychography in diffraction.

The scientific program will be illustrated with different types of experiments aiming to get insight in different research areas. They are based on the current knowledge/experience but profiting from the unique capabilities/performances that CoDI will provide:

- ## Semiconductors

There is a need for a technology paradigm shift in the semiconductor industry as information and communication technologies face unprecedented technological challenges for maintaining its growth rate levels into the next decade, when new market opportunities such as artificial intelligence (AI), internet of things or edge computing are expected to further accelerate growth. These challenges arise largely from approaching fundamental limitations in semiconductor technology (including physical dimensions) and from the necessary improvements in the energy efficiency with which information is processed, communicated, and stored. Without a quantum leap in terms of chip energy efficiency, the integrated circuit power consumption generated, for example, by Internet traffic, will lead to a significant increase in the overall energy consumption and put the maximum global warming target in jeopardy. Only with the help of new chip technologies such as neuromorphic or quantum computing, a significant improvement in terms of energy consumption per computing task will be achieved. Disruptive breakthroughs are needed in the areas of materials, device structure and related processes, architectures, systems and software.

Healthcare and life sciences are also key due to the aging population in developed countries and the broad adoption of semiconductor technologies, both for data-capture in form of intelligent sensors and actuators, as well as in terms of the usage of patient data in combination with AI. In the case of intelligent sensors, new technologies and materials like two-dimensional, highly sensitive graphene layers are opening new application spaces like neurotechnologies.

Last, but not least, industrial markets and applications are also undergoing a huge transformation, mainly driven by environmental reasons, since some of them belong to the biggest polluters and there is a strong pressure from regulators to adopt clean energies (solar, wind, green hydrogen, etc.) in combination with robotics and efficient solutions.

As dimensional scaling of CMOS will eventually approach fundamental limits, new information processing devices and architectures for both existing and new functions need to be explored and developed. This is the driving interest in new materials and devices for information processing and memory, new technologies for heterogeneous integration of multiple functions, and new paradigms for system architecture. While some of these technology solutions will likely be integrated on a Si-based platform, the vast majority of the newly developed “beyond CMOS” technologies will be based on entirely new materials and physics. To deliver these capabilities, enhanced metrology will be needed to accelerate material evaluation, improvement, and capabilities.

ALBA offers a suite of advanced characterization tools allowing to visualize the structure of matter and at the same time to measure its electronic states, including local effects and the band structure itself. The combination of atomic resolution, chemical sensitivity, and high penetration power makes this toolbox indispensable for the development of devices, especially when new materials and material combinations are employed. Three-dimensional high resolution non-destructive imaging with spectroscopic specificity and high penetration depth as offered by CoDI beamline will be a key addition in the field of chip science and technology. CoDI can substantially contribute to developing fabrication processes for optimizing performance as well as production yield, to verify designs of third-party purchased chips by non-destructive imaging of devices and integrated circuits, for device performance characterization, and quality assurance. Combined with functional sample environments for *operando* characterization, it has enormous potential for understanding material growth and transformation during post treatments such as tempering, irradiation, or implantation as well as for the study of device degradation under working conditions.

The global chip shortage which started in early 2020 has turned public attention to the semiconductor technology, underscoring the huge impact of this industry on the global economy and highlighting the urgency of taking further steps. The EU plans to invest €43 billion in the frame of the EU Chips Act, and the Spanish PERTE initiative plans for a €12,3 billion investment in order to stimulate the semiconductor technology industry in the short-term, and the economy as a whole in the mid- and long-term.

BCN-InnoFab is a proposal within the PERTE frame to build an advanced semiconductor fabrication and characterization facility in the ALBA campus in order to contribute to the development of emerging devices and novel architectures, to identify and resolve the scientific/technological challenges gating their acceptance by the semiconductor industry, to mature their technology readiness level and to, ultimately, drive breakthrough advances in future manufacturing technology.

Based on the analysis of the opportunities offered by market drivers and of the capabilities of the surrounding ecosystem, InnoFab will focus on transformational materials, processes and devices that can provide new capabilities or functional enhancements in application areas including:

i) Energy-efficient processing.

ii) In-memory computing.
iii) Neuro-inspired/mimetic computing.
iv) Quantum computing.
v) Analog electronics for world/human-machine interfaces.

In particular, InnoFab will focus on classes of semiconductor/microelectronic materials exhibiting properties such as high charge mobility, ferroelectricity, phase transitions, resistive switching, or superconductivity. Examples of these materials classes are:

- Two-dimensional (2D) layered materials (graphene, transition metal dichalcogenides),
- Thin film oxides (complex oxides, transition metal oxides, ferroelectric, phase change),
- Thin film superconducting materials (for superconducting qubits).

InnoFab will provide advanced prototyping and scale up capabilities to address the broad needs of the emerging transformational semiconductor and microelectronics technologies and processes related to devices such as

1. High mobility BEOL transistors,
2. Beyond-Boltzmann transistors (FeFETs, non-Si FinFETs, etc),
3. High performing non-volatile memories (RRAM, STT-MRAM, PCRAM, FeRAM),
4. Neuromorphic processing devices: 2 terminal (RRAM, SOT-MRAM, PCRAM, FeRAM) and 3 terminal (FeFET, 2D mem-transistor, etc.) synaptic devices,
5. Sensors and actuators for flexible electronics and advanced brain-computer technologies,
6. Superconducting & semiconducting qubits and technologies.

InnoFab will also offer processes and metrology for heterogeneous integration, combining unconventional materials and processes with Si-CMOS technology.

CoDI will contribute to these developments by providing a portfolio of cutting-edge characterization techniques on the nanoscale[1,2]. Bragg-ptychography will allow strain mapping of buried layers and devices with a spatial resolution in the 10 nm range. The ability to work without destructive sample preparation such as thinning or polishing is key in order to preserve the strain state, which is carefully engineered in order to modify material parameters such as electron mobility with direct impact on device performance. Imaging of heterogenous systems in 3D will enable for example assessing the integrity of interconnects in operation conditions, critical for System-in-Package integration, or for verification of third party delivered components in order to detect unwanted integrated functions. It will be possible to measure volumes of about 500 x 500 x 5 μm^3 at a resolution of 15 nm in about 20 hours, or a small volume of 10 x 10 x 10 μm^3 with 6 nm resolution in 1h [1,5]. For this purpose, we will use holo-tomography and/or ptychographic tomography in combination with the two available nano-focus beams of about 30 nm and 6 nm provided by the KB mirrors and the MLLs, respectively. Working at the focal plane, XRF will provide elemental maps of the samples in 2D and 3D, which is relevant e.g. to study interdiffusion even under operation or growth conditions or e.g. during postgrowth thermal treatments, with a resolution limited by the focus size.

We propose to build CoDI and InnoFab adjacent and interconnected to each other. The integrated design of InnoFab and the ALBA upgrade brings unprecedented opportunities to develop specific and optimized services for solving burning challenges during development and production in a fast and cost-effective manner. It provides significant advantages in providing a secure and confidential environment for proprietary developments, hard to find in standard user facilities and essential if trade secrets are in the focus, in delivering the timely provision of data adjusted to the production needs, in opening the toolset for quality assurance and inspection purposes, and in developing multimodal characterization approaches within a production environment. This unprecedented synergistic partnership brings not only technical advantages but also the chance to customize the access and support policy and to profit from extended networking opportunities.

- **Catalysis**

The design and study of advanced electroactive materials and their application for the development of more efficient and durable electrochemical devices, including fuel cells, electrolyzers and batteries as the most representative systems, represent a major challenge for the scientific community and are the subject of very valuable contributions. The development of such electrochemical devices would strongly contribute to the desired decarbonization process. For a better understanding of the behavior of these electroactive materials and electrochemical devices, the use of *in situ* and /or in *operando* studies becomes essential. In this respect, CoDI will significantly contribute to visualize and understand the properties of these electroactive materials and the performance of electrochemical devices under working operation conditions. To illustrate the possibilities, we describe in the following, two relevant and recent scientific cases related to the topic.

#1. Understanding structural degradation in Li- and Mn-rich (LMR) cathode materials.

Li- and Mn-rich (LMR) materials are relevant electroactive systems that can be used as cathodes and can significantly improve battery energy density. However, it is also known that these systems suffer voltage fades whose origin remains still under discussion. Although lattice displacement and nanoscale strain are relevant parameters in batteries, the lack of convenient characterization tools has not allowed to properly understand the key role of these parameters during electrochemical reactions. Very recently, *in situ* Bragg-CDI measurements have been used to visualize lattice displacement and analyze strain evolution of LMR primary particles under relevant electrochemical conditions [3]. The *in situ* Bragg-CDI measurements were performed at the 34-ID-C beamline of the Advanced Photon Source (APS) using 11.2 and 9 keV monochromatic beams in two independent experiments. The coherent X-ray beam was focused using two KB mirrors to approximately 1 × 1 μm^2 illuminating the LMR nanocrystals. The experiment was done on 10 μm thick LMR electrodes in transmission geometry. From the fringe spacing in the diffraction patterns, they estimated that the particle size of the LMR is approximately 600 nm Thanks to the *in situ* nanoscale sensitive coherent X-ray diffraction imaging technique, they showed that nano-strain and lattice displacement accumulate continuously during operation of the cell and that this effect was the driving force for both structure degradation and oxygen loss. These structure degradation and oxygen loss seems to be the origin of the rapid voltage decay in LMR cathodes. Fig. 1 shows some of the representative Bragg-CDI results included in the [3].

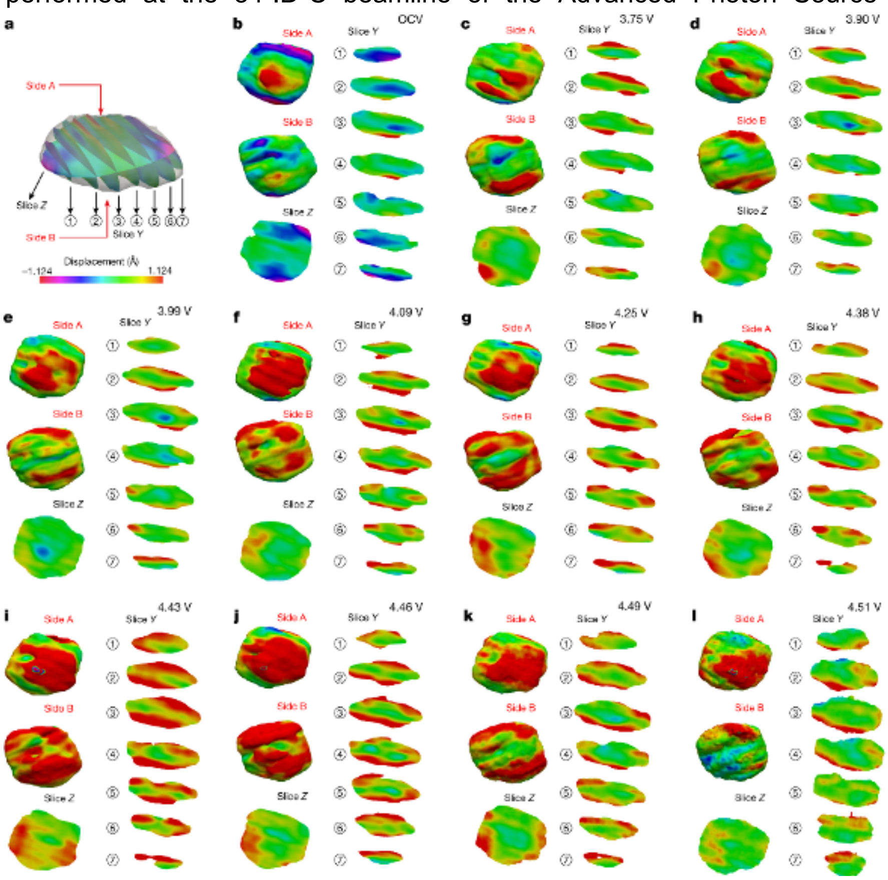

Figure 1. In situ (a) Bragg-CDI images of a 3D LMR particle in the strain field, measured at 3.2 V (OCV) (b), 3.75 V (c), 3.90 V (d), 3.99 V (e), 4.09 V (f), 4.25 V (g), 4.38 V (h), 4.43 V (i), 4.46 V (j), 4.49 V (k) and 4.51 V (l). The compressive and tensile strains are visualized by blue and red colours, respectively. The strain evolution in each state is detailed by the spatial location of the slices along the y axis [Extracted from 3].

CoDI will allow Bragg-CDI experiments to study processes in 4D (3D + time). In addition, the small focus (< 50 nm) would allow the study of smaller particles. Also, shorter measurement times will be possible. CoDI will offer the possibility to operate with focuses optimized for energies in between 10–30 keV.

#2. Imaging the strain evolution of a platinum nanoparticle under electrochemical control.

Despite Pt nanoparticles (NPs) have been applied and studied in innumerable (electro)catalytic systems, the development of more advanced *in situ* or in *operando* characterization methods represent a great opportunity to get more insight on the understanding of the properties of these Pt NPs under relevant working conditions. In this sense, it is well established that by modulating surface strain, the chemisorption energies of adsorbates on active sites can be conveniently tuned and, consequently, the kinetics of (electro)catalytic reactions enhanced. This also applies in gas phase catalysis. *In situ* Bragg-CDI has demonstrated to be a powerful tool to acquire 3D strain maps of NPs and nanostructures. Very recently, Atlan et at. illustrated the potentialities of the Bragg-CDI approach to map and quantify strain within individual Pt catalyst NPs under electrochemical control [4]. These experiments were carried out at the ID01 beamline of the European Synchrotron Radiation Facility. The Bragg-CDI measurements were performed with a photon energy of 13 keV and the beam size was focused down to 690 nm (horizontally) × 630 nm (vertically). The diffracted beam was recorded with a 2D Maxipix photon-counting detector (pixel size 55 × 55 μm^2) positioned at a distance of 0.87 m. They measured 002 Pt Bragg reflection in three dimensions by rotating the particle around the Bragg angle (16.12°) through 1°, in steps of 0.0125° with a counting time of 0.2 s per point and total flux of about 1.4×10^{12} counts s^{-1}μm^2. The detector was positioned at an out-of-plane angle of around 28°. The timescale of one Bragg-CDI measurement was approximately 10 min. Fig. 2 shows some representatives Bragg-CDI results in which the influence of the electrode potential on surface strain can be visualized.

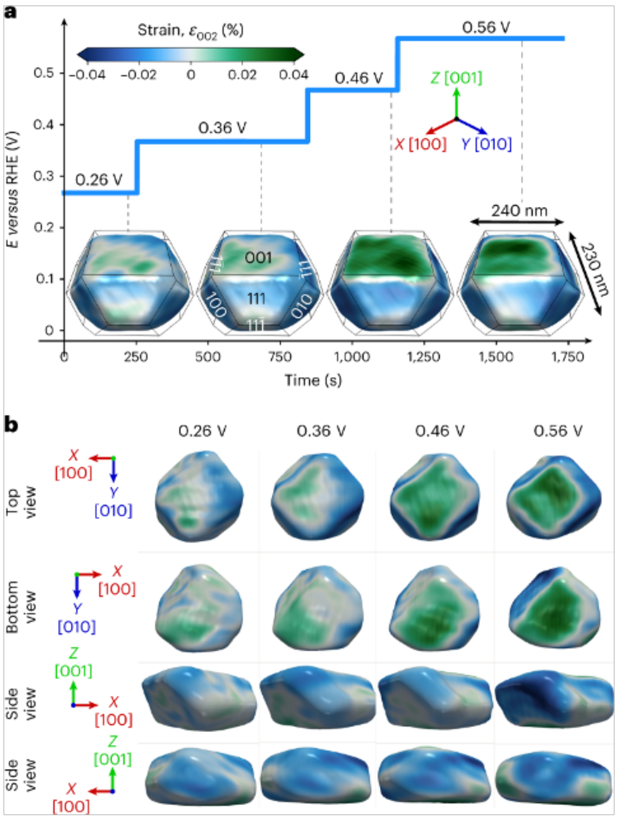

Figure 2. Influence of electrode potential on surface strain, a, Evolution of the strain at the surface of the Pt particle at varying electrode potentials. b, The same particle viewed from different perspectives. Colouring is identical in both a and b. Extracted from [8].

By combining *in situ* 3D strain microscopy with nanometric resolution, with density functional theory and atomistic simulations, the heterogeneous nature was observed including potential-dependent strain distribution between highly coordinated ({100} and {111} facets) and undercoordinated atoms (edges and corners). Strain propagation from the surface to the bulk of the nanoparticle was also shown. This information is very valuable and can significantly contribute to the design of more efficient strain-engineered nanocatalysts for energy storage and conversion applications.

Due to the small focus (< 50 nm), CoDI in the ALBA II will provide the opportunity of studying smaller Pt NPs and more similar than those used in practical applications. In this respect, Bragg-CDI of single 20 nm Pt particles has been performed at the ID01-EBS beamline of ESRF [12]. The long working distance at CoDI will allow to combine spectroscopy and imaging at high pressure not reachable at electron microscopes. The laser available at CoDI will contribute to perform *in situ* excitation of photocatalytic systems in gas atmosphere and study these processes with nanometric resolution.

- ## Quantum materials

Inhomogeneity at the nanoscale is intrinsic in quantum materials. During phase transitions domains on this length scale naturally occur in correlated materials, and novel emergent phases that are not stable at the mesoscale have also been observed [13]. Most existing techniques do not provide bulk sensitivity and thus do not report on the full domain structure. Imaging phase separation at the nanoscale using coherent imaging has recently been achieved using soft X-rays both for thermal [14] and light-driven phase transitions [15], but these experiments rely on X-ray absorption contrast and thus report primarily on the electronic structure. The complementary technique of scanning near-field optical microscopy (SNOM) also reports primarily on electronic structure and is not bulk sensitive[16]. However, phase transitions in quantum materials also involve structural symmetry breakings, and often exhibit extreme sensitivity to strain. As such methods that can directly image structural inhomogeneity in quantum materials, ideally correlating them to electronic changes and the presence of defects, are needed. The 20 nm resolution offered for nano-XRD and nano-XRF measurements at CoDI will be a powerful tool for visualizing many of these structural transformations, but for moving beyond 10 nm resolution, imaging strain fields, or for *in situ* measurements alternative approaches are required. Coherent diffractive imaging in the hard X-ray has long been posited as the solution to this problem[17], but has yet to be realized due to the challenges in preparing samples of quantum material and measurements under cryogenic or *operando* conditions. Tele-ptychography [1] gives the CoDI beamline the capabilities to perform *operando* studies on samples addressed by strong fields or undergoing systematic temperature scans where scanning methods may struggle, and will enable coherent structural measurements, along with correlations to X-ray spectroscopic characterization, while additional femtosecond laser sources can drive the generation of non-equilibrium phases that at CoDI could be studied with sub-ns resolution.

Nanoscale Phases and phase transitions

There are numerous claims in the literature of the emergence of the novel phases at the nanoscale in quantum materials that cannot be stabilized at the meso or macro-scale. For instance, in V_2O_3 SNOM measurements claim that an intermediate phase emerges at the nanoscale during the insulator to metal phase transition at 180K [18], in strained manganite films optical excitation has been shown to induce nanoscale domains of an emergent ferromagnetic metal in an antiferromagnetic insulating matrix [19], amongst others, but direct nanoscale structural determination is lacking in most cases. This is particularly challenging for studying phase transitions, where scanning temperatures while maintaining alignment can be challenging, or large applied fields prevent nearby scanning probes. Most measurements additionally lack depth-resolution due to their low photon energies (optical or SXR), which can strongly change domain structure, as already epitomized in the radically different physics in low-dimensional materials. CoDI will enable the 3D structural characterization of these transitions at their characteristic nanometer scale, while correlated spectroscopy data will allow links to the resulting electronic properties.

Operando Transitions

Driven quantum materials are being extensively explored for next-generation nanotechnology, for example with neuromorphic computers or memtronics from phase-change materials. Current driven transitions in the quantum material VO_2 has been extensively explored for these applications, see Fig. 3, where a variety of complex memory effects have been observed that make it appropriate for neuromorphic computing [20], but to understand these effects accurate characterization of the domain structure and phase transition in *operando* is required. Recent advances have enabled nano-imaging of the electronically induced phase filaments [21,22], but acquisition times on the order of several hours are prohibitively slow for characterization of stochastic and memory processes, which may require many hundreds of repetitions to map. In addition, these prevent mapping the dynamics of the filament and domain formation, which can occur over tens of microseconds when electrically driven [23] or on picosecond timescales when optically driven [24]. The estimated two-order-of-magnitude of flux improvement at CoDI will enable *in situ* characterization not only of simple voltage filament devices, but more complex neuromorphic computing circuits and uncover the nanoscale origin of the memtronic effects in VO_2 and other quantum material-based devices.

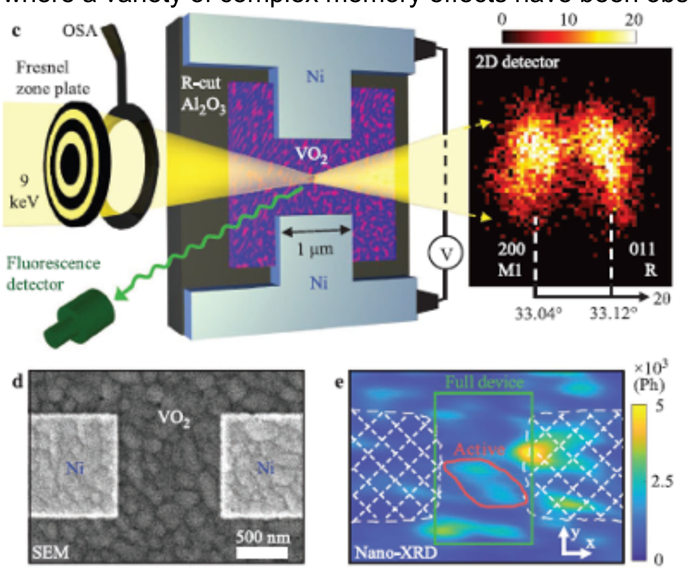

Figure 3: XRD nano-imaging of current induced phase filaments in VO_2. SEM images (d) and rutile phase maps (e) show a strong effect of topography upon the filament patterns. Adapted from 19.

- **Earth and Planetary sciences**

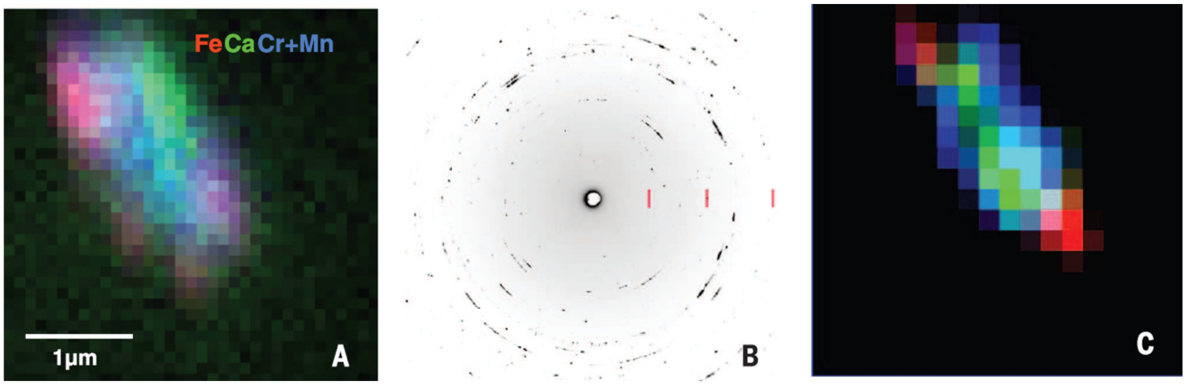

Figure 4: Combined nano-XRF and nano-XRD measurements collected on IDPs grains at ID13 (ESRF) using a 200 nm X-ray beam (A)Tri-color iron, calcium, chromium + manganese elemental map derived from XRF data; (B) XRD pattern taken at 13.9 keV (λ=0.8923Å); (C) phase map indicating olivine (green), spinel (red) and unidentified phase (blue).

Earth and Planetary materials are most often highly heterogeneous and may contain sub-µm mineral inclusions that are very informative about physico-chemical processes that have occurred deep in the Earth mantle or in planetary bodies. Therefore, nano X-ray beam studies are valuable to disentangle such complex landscapes. X-ray base synchrotron techniques can be applied with high spatial resolution, including nano-XRD, nano-XRF and coherent X-ray imaging techniques. By applying these methods at multi-length scale in conjunction with a fast-readout area detector, they permit efficient mapping of possible host regions in earth and planetary samples. Such samples may bear materials from the Earth and Moon, Mars and from a wide variety of smaller bodies such as meteorites and materials recovered from asteroids and comets. Their minor and trace elements as well as isotope composition and crystal structure provide important insights into the geochemical cycling of elements and can give us information about the origin and evolution of the Earth and solar system.

#1. Evidence for interstellar origin of dust particles. Interplanetary dust particles (IDPs) are being collected in the stratosphere, from terrestrial polar ices, deep-sea sediments, and within impact features on spacecraft [25,26].

Recent investigations on a few IDPs grains brought back to earth by the Stardust NASA mission have provided the first quantitative compositional information of contemporary interstellar dust crossing the solar system [27]. The example included in Fig. 4 shows how combined nano-focus synchrotron techniques can be used to determine chemical composition and structure of interplanetary samples with particle size in sub-µm range (grain size of 0.2-2 µm). The particles had a significant crystalline fraction revealing olivine silicate phase, a mineral usually found in the Earth mantle, together with spinel and nanophase iron inclusions confirming that these interstellar particles diverge from any representative model inferred from astronomical observation and theory.

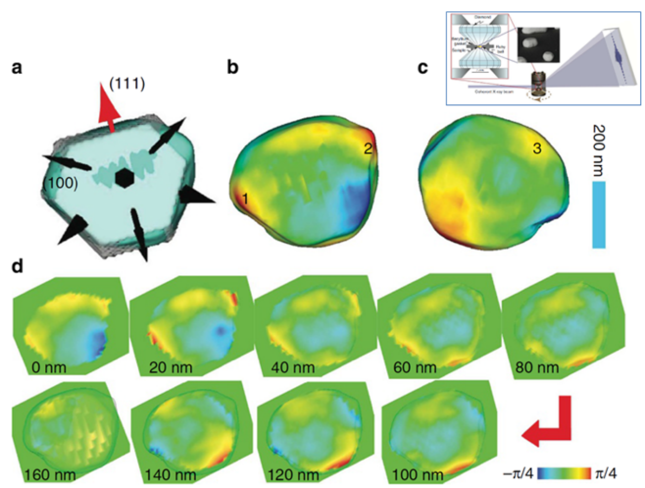

Figure 5. (A) 3D morphology and strain distribution of gold nanocrystal under pressure. Snapshot at 1.7 GPa showing the isosurface of the reconstructed amplitude superimposed to the normal directions of {111} and {100} crystal planes. Top (B) and bottom (C) view of phase shift distribution pasted on the 30% isosurface plot. (D) 3D phase distribution at different slicing depths spaced by 20 nm steps from top to bottom. (Onset) typical experiment setup for CXDI performed at 34-ID-C (APS) using a coherent 10.8 keV X-ray beam focused at 1 µm (FWHM).

#2. Nanoscale strain evolution under high pressure. The deformation of Earth materials subjected to stress buildup or strain localization relies on understanding the geodynamic processes over a large time scale under extreme conditions [28]. Relevant studies on morphology evolution and internal strain of Earth materials under pressure give insights into structural stability and deformation mechanism. Such mechanism probed by individual nano-grains under extreme conditions has been studied by Bragg-CDI technique, where a coherent X-ray beam illuminates the sample in a diamond anvil cell while the nanocrystal inside is aligned to the rotation center to allow 3D phase retrieval (onset of Fig. 5). The shape and internal strain distribution after plastic deformation in a 400 nm gold sample is shown in Fig. 5 [29]. In this way the 3D morphology and strain evolution under compression were shown with a good spatial resolution of 30 nm and 10^{-4} strain sensitivity. This allows it to shape evolution at various pressures corresponding to the single crystal rheology as activated dislocations are created and pass through the nanocrystal while strain evolution indicates the local lattice distortion.

The nano-focused beam(s) at CoDI will allow experiments with improved spatial resolution and to combine the nano-XRF elemental studies with coherence-based 3D X-ray imaging.

• Geochemical dissolution and precipitation processes.

The understanding of dissolution and precipitation processes at the nanoscale is very limited although of high fundamental interest and immense industrial relevance. This is due to the lack of methods that can image these processes with (simultaneous) enough spatial-resolution, time-resolution, component-contrast and field of view. Dissolution-oversaturation-precipitation processes take place in fields as diverse as minerals in geochemistry, cements in building materials, biogenesis or biomaterials in health, etc. Next we present two scientific cases where CoDI will contribute to understand the dissolution processes in 4D in relevant conditions.

#1. Enhancing hydration and strength development of low-carbon cements.

Portland concrete is the world's largest fabricated commodity, ~20 billion tons/yr. The enormous production of Portland cement (PC), ~4 billion tons/yr, results in ~2.7 billion tons/yr of CO_2 emissions. If cement production is considered a country, it would be the third emitter after China and USA. Therefore, there are many attempts to decrease the cement CO_2 footprint. Sustainable, economically-feasible low-carbon cements are the hottest topic in cement research. The main drawback of low-carbon cement proposals is their slow hydration kinetics in the first 3 days. In order to rationally design approaches to decrease the embodied carbon content of binders, maintaining the performances, cement hydration understanding is key. Unfortunately, there are several key unanswered questions regarding the complex dissolution and precipitation processes at the nanoscale that lead to the early hardening of cements.

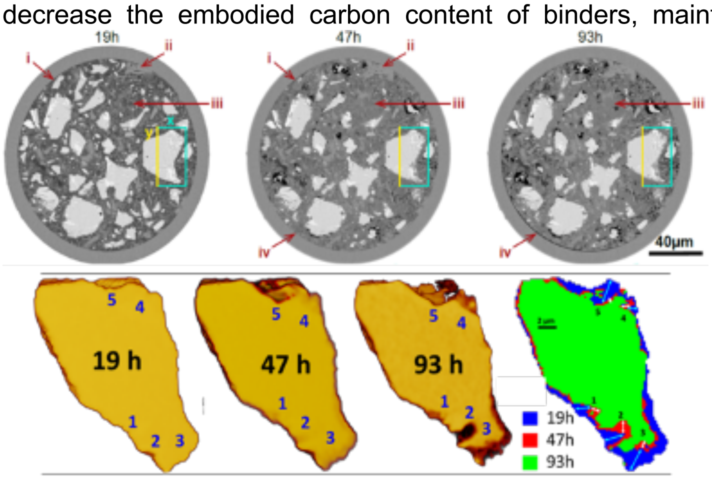

Figure 6. 4D nanoimaging for a PC paste by near-field PXCT. (Top) Orthoslices showing: i) dissolution of cement grains, ii) portlandite growth, iii) C-S-H gel densification, and iv) chemical shrinkage. These features are labelled with red arrows. (Bottom) 3D representation of a segmented alite particle, size ~10 mm, showing the evolution of the etch-pits and the procedure to estimate the key descriptor: etch-pit growth rate. The current spatial resolution is fine for visualizing etch-pit growth, but not for accurate rate quantification as function of time and alite initial particle size. [Adapted from 6].

In a recent work by some members of CoDI proposal [6], we adapted near-field ptychographic X-ray CT (PXCT) for *in situ* 4D cement hydration studies. The measurements were carried out at cSAXS (SLS) BL in a high-stability instrument in air, E=8.93 keV. The thickness of the capillary was 160 µm and it was scanned with a FOV of 186 µm in order to have about 10 µm of air at both sides of the capillary for all projections, which is required for quantitative electron density phase imaging. The coherent illumination was defined with a Fresnel zone plate (FZP) which, at this energy, had a focal distance of 51.9 mm. The flux at the sample position was ~2×10^8 photons/s. The sample was placed 13 mm downstream the focus, i.e. near-field condition, where the illumination had a size of ~30 µm. Scans were recorded following a Fermat spiral with an average step size of 7 µm . At each position, magnified images were recorded with an in-vacuum Eiger 1.5M detector, pixel size=75 µm , placed 5237 mm downstream the sample, yielding a voxel size of 186.6 nm. The resulting spatial resolution was ~250 nm. The single image acquisition time was 0.1 s and a scan speed of ~5 Hz was achieved by a combined motion of the FZP and the sample, while having an effective static illumination on the sample during acquisition. Just 420 projections were taken at equal intervals from 0 to 180 deg, resulting in a 3 h tomogram, scanning only 30 µm in height. Fig.6 shows some key results from [6]. It is noted here the importance of using near-field ptychography for attaining very high-quality data with quantitative contrast in reasonable acquisition times.

Many nanostructural details have been obtained including alite spatial dissolution rate and C-S-H gel shell characterization. However, this work is limited by long total acquisition times, ~3 h, that it could be decreased down to 30 min at CoDI if the coherent flux is larger than 10^{10} photons/s, and if radiation damage is not important, or it can be minimized by fast acquisition and advanced denoising. Moreover, the spatial resolution should be decreased to ~100 nm, hence, smaller etch-pits in smaller alite particles could be mapped out, which are key for understanding and accelerating the early age cement hydration. In near-field PXCT, if a sufficient number of projections are recorded, the spatial resolution is limited by the magnified pixel size, which is determined by the pixel size of the detector, the sample-detector distance, the divergence of the illumination and the focus-sample position distance. Hence, the detector will be placed as far away from the sample as possible. CoDI should allow distances as large as 20 m, if the pixel size of the detector is kept constant, i.e. 75 µm, for attaining the target spatial resolution. The optimized beam energy of CoDI, 10-30 keV, will allow thicker samples, i.e. to move beyond the current limit of 200 µm towards 500 µm, making a relevant impact in low-carbon building materials development. It must be underlined that fast mass dissolution at early PC hydration ages could blur the images in the (relatively long) ptychographic (scanning) approach. If this is the case, CoDI will allow to switch to holotomography that should also yield very high resolution with shorter overall recording times. This full-field technique requires the acquisition of 3-4 tomograms with variable sample-detector distances, all within the near-field regime. In this case, the sample is placed at variable distances in the divergent beam. This X-ray imaging example illustrates the complementarity and versatility of CoDI, as proposed.

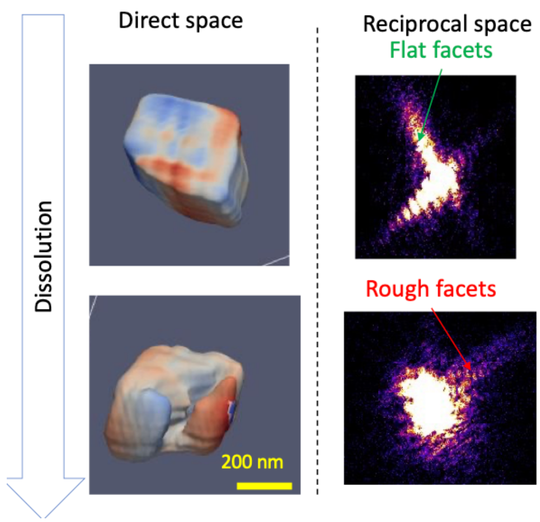

Figure 7. Sensitivity of coherent X-ray patterns to the morphological transformation of a calcite nanosized crystal upon dissolution.

#2. Growth and dissolution of minerals under realistic conditions.

Growth and dissolution, two primary forms of chemical reactivity of mineral-water interfaces, ubiquitous at and below Earth's surface, is a critical process whose understanding underlies our ability to develop quantitative and robust predictive models for a wide range of geological and environmental issues related to elemental transport in aqueous environments. However, the strong impact on the reactivity due to the structural complexity of mineral-water interfaces, including irregular 3D morphologies, exceeds that which can be understood with normal incoherent scattering tools (e.g., X-ray reflectivity, electronic microscopy, etc.).

To date, most of the *in situ* interface dissolution/crystallization studies have been performed with AFM on extended and flat cleavage planes of single crystals, whose chemical reactivity differs from 3D crystals. In fact, the observation of highly inhomogeneous dissolution rates at the surface of a 3D calcite crystal with *ex situ* measurement of X-ray nano-tomography, reveals the strong connection between reactivity and surface morphology, with varying chemical reactivity for terrace, corners and edges. However, these techniques are blind to the existence of other internal structural features such as atomistic defects or strain fields whose role in the chemical behavior of the nanosized crystal remains invisible. Bragg-CDI and Bragg-ptychography are ideally suited to image irregular 3D mineral interfaces (see Fig. 7) achieving nanometric resolution of internal defects and associated strain fields. While Bragg-CDI is better suited for nano-sized crystals, Bragg-ptychography can image wider fields of view spanning up to few µm. Bragg-CDI has been successfully applied to study the role of screw-dislocations upon growth or dissolution, while Bragg-ptychography can image stacking faults in nanowires within 10 nm resolution. For both techniques there has been a great effort in increasing their flexibility for in situ experiments by designing new algorithms and methods [30-33]. Despite all this work, most of the Bragg-CDI/ptychography measurements of mineral-water systems have been performed only on static samples and ex situ due to its slow data acquisition rate (of the order of minutes).

CoDI will provide a great opportunity to design new approaches of Bragg-CDI and Bragg-ptychography to visualize processes in 4D. Very specially, the intense coherent flux (of at least 10^{11} photons/s at the sample position) and the small focus (sub-50 nm) achieved with the KB mirrors or (around 6 nm) with the MLLs will enable the implementation of a new approach of Bragg-CDI which reduces the measurement time by factors between 5 and 10 (depending on the size of the crystal and the environment). In the context of a collaboration with V. Chamard and M. Allain (Institut Fresnel, France), I. Calvo, member of CoDI proposal, has performed numerical simulations which show that under specific illumination conditions, the oversampling ratio (OSR) constraint along the rocking curve direction can be relaxed. Thereby, the simulations suggest that we can reduce the number of diffraction patterns required to retrieve a 3D image of the crystal without degrading the reconstruction quality, and hence, increase the measurement rate. Furthermore, these advances can also be applied to Bragg-ptychography, in order to study larger mineral interfaces in the µm length scale. Finally, CoDI will offer the possibility to operate with a focus optimized for energies in between 10–30 keV. This is an important asset for *in situ* experiments since we will be able to follow the crystallization or dissolution of crystals inside large volumes of liquid environment(s). It also will reduce the beam damage by diminishing the scattering cross section. It is noted that at CoDI the beam size will range from 6 to 200 nm, hence only crystals smaller than the beam size will be investigated by Bragg-CDI, until the ptychographic approach is implemented in a subsequent step.

- ## Magnetic Nanoparticles in Biological systems

CoDI will emerge as a powerful and unique characterization instrument within the available ALBA II beamlines for addressing various issues and societal challenges related to the use of NPs with different potential applications in fields such as Medicine, Biology and food safety [34-39]. NPs have become, among other things, as promising drug delivery vehicles due to their ability to selectively target diseased tissues and cells, reducing the toxicity of drugs and improving their efficacy. Besides, 4d and 5d element NPs have unique properties that make them suitable for a wide range of biomedical applications, because they have high surface area-to-volume ratios, which can enhance drug loading and release, and they can be easily functionalized with targeting moieties and imaging agents. NPs also have many potential properties to improve the stability and solubility of encapsulated cargos, promote transport across cellular membranes and prolong circulation times to increase safety and efficacy. For these reasons, NPs research has been widespread, generating promising results in vitro and in small animal models. However, despite this extensive research, the number of nanomedicines available to patients is drastically below the expected and anticipated projections until now, partially because of a translational gap between animal and human studies. Despite the huge efforts, many early NPs iterations were unable to overcome the biological barriers to delivery, but more recent NPs designs have utilized advancements in controlled synthesis strategies to incorporate complex architectures, bio-responsive moieties and targeting agents to enhance delivery. NPs can therefore be utilized as more complex systems — including in nanocarrier-mediated combination therapies — to alter multiple pathways, maximize the therapeutic efficacy against specific macromolecules, target phases of the cell cycle or overcome mechanisms of drug resistance.

Experiments on CoDI are expected to boost the research on NPs contributing to their practical application and transfer to industry. The various national or international groups involved in this activity have vast experience covering NPs synthesis, both by classical and novel routes, as well as their application to point-of-care bioanalytical devices, hyperthermia, and controlled drug release. They also have extensive experience with a variety of characterization techniques and standardized nanometrology methods, which are useful for industrial utilization and enable the development of new emerging technologies that provide society with new bioanalytical tools and more efficient clinical therapies. Analysis using simple, low-cost devices has multiple applications in diagnosis, food safety, and the environment. In the clinical field, the design of new NPs could enable the development of platforms for early detection of tumors and other diseases. These tools would also be useful in the field of food safety, where pathogen detection is and will continue to be a priority.

Nowadays, one of the most vexing questions in engineered nanomaterials is how to improve disease diagnosis and treatment specificity [34]. In this respect, it is believed that NPs could help to overcome the current limitations addressed in conventional delivery — from large-scale issues such as biodistribution to smaller-scale limitations such as intracellular trafficking — through cell-specific targeting, molecular transport to specific organelles and other approaches [34]. Many types of nanomaterials (such as magnetic

NPs, metallic NPs, drug encapsulation systems, and lyophilized materials) and prototypes could be investigated using scanning coherent techniques as holotomogaphy and ptychography at the CoDI beamline as part of research projects involved in the experiments. These research outcomes could be transferable to the industry and could generate patents or new companies for commercialization. Other products derived from the research could also present high commercial interest. Many cases could be included in this scientific case, which would certainly benefit greatly. To cite a few examples: biogenic magnetite produced by magnetotactic bacteria has innate crystal perfection and biocompatibility that makes it ideal for diagnosis, therapy, and imaging techniques; phototherapy systems based on NPs or nanocomposites also evolved as an emerging hot spot in nanomedicine research, especially in cancer; also, superparamagnetic iron oxide multicore NPs are promising because recently it has been shown the significant influence of slightly different physicochemical properties on the cellular and molecular processes that define the interplay with primary neural cells, and many others [35-39]. The study of paramagnetic compounds based on 4d and 5d transition metals is an emerging research topic in the field of molecular magnetism. An essential driving force for the interest in this area is the fact that heavier metal ions introduce important attributes to the physical properties of paramagnetic compounds. Among the attractive characteristics of heavier elements vis-à-vis magnetism are the diffuse nature of their d orbitals, and their strong magnetic anisotropy.

To achieve these goals, high-resolution imaging to track the location of the relevant NPs inside the biological systems is necessary. The position system at CoDI beamline and the long working distance will allow to perform the imaging of these biological systems under high control environment parameters. This type of studies will need of a confination of high coherence scanning techniques as ptychography variants and nano-XRF for element tracing. The study of NPs *in situ* on biological tissues is important for understanding their interactions with living systems and for optimizing their performance as drug carriers. By using techniques such as tele-ptychography and Bragg-ptychography to probe the structure of NPs in *in situ* conditions, CoDI will provide information on variations in size, shape, and internal structure during their interactions with biological tissues. The possibility of using different environments for *in situ* experiments will be developed in collaboration with users. Existing environments developed for other beamlines such as FaXToR and MISTRAL will be compatible with CoDI.

In conclusion, a CoDI beamline will be a valuable tool for the study of NPs for biomedical applications. In particular, the study of 4d and 5d element NPs using CoDI could provide important insights into their interactions with living systems, improving their efficacy as drug carriers and as direct treatments.

Complex oxide thin films

Understanding emergent phases in complex and spatially inhomogeneous materials requires nanoscale imaging methods that are compatible with the relevant conditions under which they are generated and that can return information on the local spin, charge, and/or lattice state [14]. Coherent scattering methods such as CDI and ptychography have obvious advantages in front of other microscopy techniques. They can achieve diffraction-limited resolution down to nanometers, in contrast with other X-ray imaging methods (that can only achieve the same nanometer resolution when the optics is few millimeters close to the sample) [40]. Besides, they are non-destructive techniques, in contrast with electron microscopy in which complex sample preparation is necessary. Moreover, the reconstruction by numerical methods of the diffracted wavefront can be extremely useful to study in detail different aspects in a wide variety of complex oxide thin films.

Accurate characterization of ferroelectric domains in thin films at nanometer length scales is crucial for comprehending local behavior in ferroelectric materials and to integrate them in functional devices. Traditionally, this characterization has been achieved using piezoresponse force microscopy (PFM), but its resolution is limited by the tip radius, typically in the tens of nanometers [41]. At CoDI by combining Bragg-ptychography with *operando* capability, an unprecedented platform would be established for investigating the evolution of ferroelectric domains in thin films. This innovative approach would offer a quantitative, high-resolution method to gain insights into the behavior of ferroelectric materials at the nanoscale [42].

It can be envisaged that on the search for giant responses of materials, martensitic-like materials are going to be of paramount importance. Examples include materials at the verge of a diffusionless shear transition between crystallographic phases of different symmetry [43]. The transition is typically driven by temperature or composition and leads to nucleation and persistence of one phase within the other, as observed at the morphotropic phase boundary in some piezoelectric materials [44], sometimes accompanied by the presence of intermediate phases so called adaptative phases [45]. In recent years, ingredients other than temperature and composition, such a surface/interface energy or ion vacancies have been claimed to be of relevance in guiding the formation of adaptive phases displaying unexpected properties. Examples include the unexpected stabilization of the ferroelectricity phase of HfO_2, that typically is obtained when crystalline sizes of a few nanometers are embedded within a non-polar matrix [46] In the same vein, the presence of distinct nano phases are thought to be at the root of colossal mechanical, magnetic and dielectric responses observed in various materials. Deeper knowledge of the structural features at nanoscale in these “intrinsic composites” should allow to understand and boost emerging functionalities of unpredictable relevance.

The characterization of strain fields by means of diffraction coherence techniques, such as Bragg-CDI or Bragg-Ptychography, must help to discern not only how the strain induced by substrate relaxes and how this relaxation modulates the properties across the films, but also around dislocations, or at grain boundaries and domain wall between crystallographic domains. Through precise measurements and analysis, we can discern the strain distribution and its evolution at the nanoscale. This information is invaluable for optimizing material synthesis and enhancing the performance of nanodevices [47].

Beyond this, direct application of diffraction with high spatial resolution is extremely useful in complex oxide thin films characterization. A clear example of this is the study of ferroelastic domains. The spatial resolution proposed for CoDI will allow the study of single ferroelastic domains to find the true (instead of an average) symmetry/structure [48]. Even useful information concerning the domain or phase boundaries could be obtained [47]. Another example is the possibility of characterizing the structural evolution/changes in working devices in between electrodes separated by few µm, or in regions under certain illumination conditions. A third example would be the possibility of studying the structural changes in the close vicinity of local or extended defects like edge/screw dislocations, inclusions, microcracks, …

Free-standing oxide membranes are also a promising field of application of the proposed beamline. The competition between surface-induced effects and the mutual strain between ferroelastic domains, when the substrate induced epitaxial strain is absent, induce intriguing phenomena like strong change in domain wall kinetics and ripples at the mesoscopic length scale [49]. Flexoelectricity in free-standing membranes is another important topic that would exploit the great capabilities of CoDI beamline. The study of the strain gradients inducing the flexoelectric behavior in the degree of spatial resolution achievable by means of the techniques available at CoDI, such as Bragg-CDI, Bragg-ptyhography and tele-ptychography in diffraction; will allow understanding the different mechanisms and designing new functional devices.

Functional specifications.

- Photon energy range: 10-30 keV
- Photon flux in sample position: 10^{11} ph/s@0.1%BW (in High degree of Coherence)
- Degree of Coherence after Secondary Source: <98% depending on SS opening
- Beam size at sample position (FWHM):
  - No Optics: 570 x 336 µm^2.
  - KB mirrors 1[Optimized at 25 keV]: Diffraction limited, sub-50x50 nm^2 (e.g. 32x32 nm^2 at 20 keV).
  - KB mirror 2 [Optimized at 15 keV]: Diffraction limited, sub-100x100 nm^2.
  - KB mirrors: flexible larger focus for example 200x200 nm^2 (with different slits configurations).
  - Nano optics based in MLLs with sub-10x10 nm^2 focus (e.g. 6x6 nm^2 FWHM at 20 keV).
  - Possibility of working away of focus
- Expected X-ray energy bandwidth:
  - At 10 keV (Si 111): 1 eV.
  - At 10 keV multi layer mirror: 50 eV.
- Si-drift detector:
  - Si sensor thickness 500 µm. Range of energy 1.5-30 keV. Energy resolution <200 eV FWHM and scanning capability up to 1 kHz.
- 2D photon detector area and pixel size:
  - Forward Detector: pixels size ≤ 80x80 µm^2 Active area ca. 225x225 mm^2 with sensor material GaAs/CdTe for high working energies.
  - Diffraction Detector: pixel size ≤ 60x60 µm^2. Active area ca. 100x100 mm^2
- 2D photon detector traveling/positioning:
  - Forward Detector: 0.25-20.0 m (along X-ray path direction), *in vacuo* compatible
  - Diffraction Detector: 0.5-2 m (around the sample on the robot or diffractometer arm)
- Flight tube forward detector in vacuum 10^{-3} mbar to reduce air scattering.

- Operation:
  - In air: Possible need of nitrogen flow around the sample.
  - In Vacuum: 10^{-3} mbar, for High resolution imaging setup.
- Sample temperature: 80K to 500 K. Control with a Cryostream system.
- Scanning speed: 1 kHz.
- Versatility for different environments in the sample position.

Uniqueness in relation to similar beamlines in the European and world landscapes.

CoDI will compete with nano-focusing beamlines around Europe and the world where coherent imaging techniques (such as ptychography, holography, etc.) and scanning techniques (such as XRF and XRD) are already implemented and operative. CoDI will be unique because of a new concept of instrument, more versatile for the study of *in situ* and *operando* processes with two nano-focusing setups: one aiming for the ultimate spatial resolution (sub-10 nanometers) and a second one for sub-50 nm resolution compatible with large sample environments. The uniqueness of CoDI resides in:

- Long source-to-experimental-hutch distance, which allows large working distances between the nano-focusing optics and the focus. A large working distance facilitates *in situ* and *operando* testing by relaxing the constraints to develop sample environments in which different conditions, such as pressure, gas or liquid atmosphere, and temperature, can be used to control the study of the *in situ* reactions. Usually, these sample environments have sizes between 100 and 50 mm in diameter. The working distance of CoDI of around 150 mm in between optics and focus should reduce the constraints for these types of *operando* experiments while keeping a focus sub-50 nm. Such distance is crucial for in situ and *operando* studies in the proposed fields of research. For example, this long-range working distance will allow the installation of a high vacuum chamber for performing the *in situ* growth in clean conditions of full semiconductor chips.
- Sub-10 nm focusing with highly efficient optics. We envision the use of a set of MLLs, a promising technology to reach single-digit nanometers with apertures around 100x100 μm^2. These lenses, together with the high brilliance of ALBA II, will enable one of the highest resolutions and flux densities ever achieved. However, these high-resolution lenses will limit the sample environments as typical working distances are around 10 mm.
- Photon energies maximized for 10-30 keV. This positions CoDI and ALBA II in a strategic energy scale for nano-focusing by bridging what it’s feasible at nano-focusing beamlines at small diffraction-limited storage rings (NanoMAX at MAX IV) and large storage rings like ESRF and PETRA III. This energy range is sufficient to penetrate relevant materials and sizes for materials science while keeping a nanometer resolution, see scientific cases. This will also pose a challenge regarding direct-conversion detectors. As Si detectors are not so efficient at the proposed energy range, we will require sensors based on GaAs or CdTe technologies.
- The use of a secondary source will provide a controllable focal spot size, degree of coherence, and flux for the proposed energies. This makes CoDI a highly flexible beamline that can accommodate a plethora of scanning and coherent imaging techniques with different spatial and temporal resolutions by finding a balance between spatial resolution and flux.
- Long sample to detector distance. We envision having a 20 m distance between the sample and the detector. This will enable high solid angle resolution with current direct-conversion detectors not possible in similar beamlines. Direct conversion X-ray detectors are an enabling technology in X-ray science that have revolutionized several techniques at storage rings. One of the main drawbacks of direct conversion detectors vs. indirect detectors is the pixel size. While indirect detectors can have few micrometers and sub-micrometers effective pixel sizes, current direct detectors have pixel sizes of tens of micrometers, e.g., 75 µm for an Eiger (DECTRIS) or 55 µm for Medipix-based detectors. This limits the solid-angle resolution and the spatial resolution for far-field and near-field techniques, respectively. The long sample-detector distance at CoDI will enable larger illuminations and sample sizes for far-field techniques, making the scanning faster for ptychography or relaxing the sample preparation for coherent diffraction imaging. The long sample-distance detector will also allow the improvement of the spatial resolution of the reconstructions for far-field techniques at CoDI. Additionally, a large sample-detector distance will allow the detector to cope with current limits of count rate per pixel, allowing to exploit the full available coherent flux for imaging. Regarding near-field techniques, this distance will enable the use of direct detectors

to retrieve nanometer resolution over a large field of view. Thus, it will enhance the sensitivity and contrast obtained compared to the indirect detectors mostly used for such techniques.

- CoDI will have a robust data collection based on hardware trigger, arriving at 1 kHz data collection. For top detectors in the actual market, at full acquisition rate data collection up to 1 PB/day can be achieved for a continuous use of the full detector. We expect to work in rates below this but of a similar order, of around 500 TB/day, for some type of experiments like nano-diffraction. Therefore, a data and computing infrastructures and data reduction philosophy will need to be developed to satisfy the data-intense requirements of CoDI in the case of these data collection rates, archiving the data as soon as possible to a “cold” storage to release space for new users.

CoDI shares several features with other nano-focusing and coherent imaging beamlines. Therefore, CoDI will benefit from the experience of beamlines such as cSAXS (SLS 2.0), NanoMAX (MAX IV), 3-ID HXN (NSLS-II), I13 (DLS), ID01 and ID16-A/B (ESRF), and P06 and P10 (Petra III) in the imaging of functional materials. These instruments have very reduced space for *in situ and operando*, limiting the scientific cases and the sample-detector distance does not allow for the improvement of the resolution of the reconstructed images using single photon counting detectors in techniques like holo-tomography and near-field ptychography.

Holography imaging uniqueness:

MLLs provide the possibility to retrieve coherent-holographic images with a resolution limited by the focal spot over a large field of view with direct conversion detectors. Typical parameters for state-of-the-art MLLs are i) numerical aperture 10^{-2}, i) efficiencies close to 80% per lens at 20 keV, and iii) apertures around 100 µm [50]. To understand the uniqueness of CoDI, we will discuss a potential design at 20 keV based on the currently proposed beamline parameters. At 20 keV, we expect a focus of 6x6 nm^2 with a flux of $7x10^{11}$ ph/s. For the following calculation, we will assume a detector with 75 µm pixel size positioned at 20 m from the focal spot. In order to achieve an effective pixel size of 3 nm (half the focal spot), the sample will be positioned ~10 mm from the focus position with a beam size of 10x10 μm^2. The direct beam or pupil will have a size in the detector of ~2700x2700 pixels. Thus, an state-of-the-art area detector will be sufficient to retrieve a resolution of 6 nm at 20 keV. In one second, the detector will collect almost $1x10^5$ photons per pixel over the whole pupil, assuming an efficiency of 100% and a homogeneous distribution. This will open the possibility to acquire **extremely high-sensitivity phase images with a resolution of 6 nm over 10 *µ*m in 1 second**. A whole tomogram could be measured with the Nyquist sampling (4241 projections) in approximately an hour, a speed not reached by any current imaging facility at this resolution and sensitivity. In order to ensure the stability and control of the nano-focus over 1-hour scan with MLLs, a setup will be developed similar to the existing one in the HXN beamline (NSLS-II) [51]. Furthermore, control mechanisms for thermal and mechanical vibrations will be in place. Finally, as the ultimate resolution of the MLLs is achieved over a 10x10 μm^2 field of view, one could consider moving the sample out of focus to have an overview and select regions of interest to scan with nanometer resolution. Such a holographic microscope will enable **zoom-in and zoom-out imaging**. In parallel, the MLLs will be used for fast **scanning techniques with nm resolution**.

Potential synergies with other already existing programs at ALBA.

The full synergetic nature of CoDI with ALBA synchrotron infrastructure is clear, since as declared in the ALBA strategic plan “Most urgent challenges in the world are related to health, climate change, environment and energy. Solutions require the visualization of complex systems and understanding how subsystems work together on different length scales”. Therefore, CoDI beamline perfectly suits ALBA´s mission and vision, being aligned with the 2021-2024 strategic plan on different research fields such as “*catalysis and environmental sciences”, “materials for energy-related applications” and “magnetic nanomaterials”*. ALBA boosts these research programs by providing the synchrotron and beamlines infrastructure that serves the user community, but also by increasing the capabilities with dedicated laboratories with *state-of-the-art* tools for developing a full research program, *i.e.* catalysis, batteries, high pressure and materials science associated laboratories. With this aim, ALBA will upgrade its facility towards a 4^{th} generation synchrotron, ALBA II, to provide the latest technology to the scientific community. In fact, CoDI will operate in the ALBA II facility, exploiting the new capabilities (*e.g. smaller source size, higher coherence, higher brilliance*) of the last generation synchrotron to serve the community with the latest methodology and tools to address the current and future societal challenges.

CoDI will boost the scientific and technological productivity performed at ALBA II synchrotron by providing a full range of new experimental. Following the multi-modal approach in the imaging beamlines framework at ALBA [*i.e.* MISTRAL, FaXToR], CoDI will provide a higher spatial resolution imaging capability during *in situ* and *in operando* conditions, also providing morphological and compositional information of 2D/3D structures that will expand the results obtained at other ALBA beamlines. As illustration, in the field of catalysis, which it has been always a field of prime of interest at ALBA with beamlines included in the program [*e.g.* CLAESS, CIRCE, NOTOS, MIRAS, NCD-SWEET, 3Sbar], CoDI will provide information at the nanoscale to correlate the chemical and electronic information obtained at other beamlines with the 2D/3D structure and composition. In the same way, the research for energy harvesting and storage programs developed at other beamlines [*e.g.* MSPD, NOTOS, CLAESS, NCD-SWEET, FaXToR] will also benefit from the spatial and compositional information obtained with CoDI nanobeam. Moreover, the nano-diffraction and nano-spectroscopic 2D/3D mapping/tomography capabilities will provide information at the nanoscale that no other beamline at ALBA offers now since they work in the micrometer range [*e.g.* MSPD, NCD-SWEET].

The ongoing project *In situ* Correlative Facility for Advanced Energy Materials (InCAEM) is developing the infrastructure for *in situ* and *operando* investigations combining synchrotron techniques, high resolution transmission electron microscopy at the recently implemented Joint Electron MIcroscopy Center at ALBA, and scanning probe microscopies. CoDI will play a pivotal role in closing the gap between the information provided by current synchrotron beamlines and the atomic resolution microscopies, helping to disentangle the relation between the 2D/3D structure and the material performance in applications such as catalysis and electrochemistry.

In brief, CoDI will play an essential role on ALBA II scientific portfolio by providing higher spatial resolution imaging and scanning techniques with *in situ* and *operando* capabilities. It will complement not only other existing ALBA beamlines, but also the associated microscopy platform, by providing a new tool towards multimodal and correlative analysis of 2D/3D structures in the different key research fields.

Describe potential impact of the instrument on larger national initiatives.

Within the Barcelona Synchrotron Park[1], the extension of ALBA synchrotron premises, *i.e*. ASTIP - **A**LBA **S**cience, **T**echnology and **I**nnovation **P**ark, allows the creation/hosting different infrastructures and initiatives. For a summary of ASTIP, please read the page 14 of the current ALBA strategic plan 2021-2024[2]. In a nutshell, ASTIP is foreseen as an interdisciplinary innovation hub where CoDI capabilities will naturally integrate. On the one hand, the synergies of CoDI with different initiatives, possibly including the “Proyecto Estratégico para la Recuperación y Transformación Económica (PERTE)” en microelectrónica y semiconductores[3], will naturally stem from the scientific scope of the proposal. On the other hand, there are Spanish and regional plans where CoDI could partly frame. Therefore, it is not unrealistic to foresee partial (limited) funding from such funding schemes. CoDI highlights “Planes complementarios con CCAA”. In this context, there are three plans where synergies are evident “Materiales avanzados / Advanced materials”, “Comunicación cuántica / Quantum communication” and “Energía e hidrógeno renovable / Renewable energy and hydrogen”. It is noted that Catalonia is not involved in the last one but it is heavily involved in the first two ones.

[1] https://www.barcelonasynchrotronpark.com

[2] https://www.cells.es/es/que-es-alba/transparencia/publicidad-activa/docs-planificacion/strategy_plan_2021-2024.pdf

[3] https://planderecuperacion.gob.es/como-acceder-a-los-fondos/pertes/perte-de-microelectronica-y-semiconductores

References:

[1] C. Corley-Wiciak, et al. ACS Appl. Mater. Interf. 15, 3119–3130 (2023). doi: 10.1021/acsami.2c17395
[2] S. Weber, et al. Adv. Sci. 9, 2105432 (2022). doi: 10.1002/advs.202105432
[3] T. Liu, et al. Nature 606, 305-312 (2022). doi: 10.1038/s41586-022-04689-y
[4] C. Atlan, et al. Nat. Mater. 23, (2023). https://doi.org/10.1038/s41563-023-01528-x
[5] M. Holler, et al. Nat. Electron. 2, 464-470 (2019). doi: 10.1038/s41928-019-0309-z
[6] S. Shirani et al. Nat. Comm. 14, 2652, (2023). doi: 10.1038/s41467-023-38380-1
[7] D. Dzhigaev, et al.ACS Nano, 11, 7, 6605–6611 (2017), https://doi.org/10.1021/acsnano.6b08122
[8] E.H.R. Tsai, et al. Opt. Express, 24, 6441 (2016). doi: 10.1364/OE.24.006441
[9] M. Verezhak, et al. Phys. Rev. B 103, 144107 (2021). doi: 10.1103/PhysRevB.103.144107
[10] A. Rodriguez-Fernandez, et al. Phys. Rev. Lett. 127, 157402 (2021). doi: 10.1103/PhysRevB.103.144107
[11] S. Marchesini ,Nature Photonics volume 2, pages 560–563 (2008) doi: 10.1038/nphoton.2008.154
[12] M.-I., Richard, et al. J Appl Crystallogr. 55, 621-625 (2022).doi: 10.1107/S1600576722002886
[13] D.N. Basov, et al. Nat. Mater. 16, 1077-1088 (2017). doi: 10.1038/nmat5017
[14] A. S. Johnson, et al. Sci. Adv. 7, eabf1386 (2021). doi:10.1126/sciadv.abf1386
[15] A.S. Johnson, et al. Nat. Phys. 19, 215-220 (2022). doi:10.1038/s41567-022-01848-w
[16] B.T. O'Callahan, et al. Nat. Comm. 6, 6849 (2015). doi: 10.1038/ncomms7849
[17] J. Miao, et al. Science 348, 530–535 (2015). doi: 10.1126/science.aaa1394
[18] A.S. McLeod, et al. Nat. Phys. 13, 80–86 (2017). doi: 10.1038/nphys3882
[19] J. Zhang, et al. Nat. Mater. 15, 956–960 (2016). doi: 10.1038/nmat4695
[20] M. Samizadeh Nikoo, et al. Nat. Electron. 5, 596–603 (2022). doi: 10.1038/s41928-022-00812-z
[21] S.Cheng, et al. Proc. Natl. Acad. Sci. 118, e2013676118 (2021). doi: 10.1073/pnas.2013676118
[22] A.G. Shabalin, et al. Small 16, 2005439 (2020). doi: 10.1002/smll.202005439
[23] J. Del Valle, et al. Science 373, 907–911 (2021). doi: 10.1126/science.abd9088
[24] D.J. Hilton, et al. Phys. Rev. Lett. 99, 226401 (2007). doi: 10.1103/PhysRevLett.99.226401
[25] S.K. Shearer, et al. Rev. Mineral. Geochem. 36, 1-24 (1998). doi: 10.1515/9781501508806-006
[26] T. Noguchi., et al, Nat. Astron. 7, 170-181 (2023). doi: 10.1038/s41550-022-01841-6
[27] A.J. Westphal, et al. Science, 345, 786-791(2014). doi: 10.1126/science.1252496
[28] N. Hilairet, et al. Science, 318, 1910-1913 (2007). doi: 10.1126/science.1148494
[29] W. Yang, et al. Nat. Comm. 4, 1680 (2013). doi: 10.1038/ncomms2661
[30] I. Calvo-Almazán, et al. Sci. Rep. 9, 6386, (2019). doi: 10.1038/s41598-019-42797-4
[31] I. Calvo-Almazán et al., IEEE J. Photovoltaics, 9, 1790-1799 (2019). doi: 10.1109/JPHOTOV.2019.2942487
[32] I. Calvo-Almazán and P. Fenter, New J. Phys. 23, 073018 (2021). doi: 10.1088/1367-2630/ac0d2d
[33] M. Hill, et al., Nanolett. 18, 811, (2018). doi: 10.1021/acs.nanolett.7b04024
[34] M.J. Mitchell, et al. Nat. Rev. Drug Discov. 20, 101-124 (2021). doi: 10.1038/s41573-020-0090-8
[35] E. Benayas E, et al. ACS Appl. Mater. & Interf. 15, 17726-17741 (2023). doi: 10.1021/acsami.3c02729
[36] J. Li, et al. Bioactive Mater. 23, 471–507 (2023). doi: 10.1016/j.bioactmat.2022.11.013
[37] M. Souri, et al. Drug Deliv. 30, 2186312 (2023). doi: 10.1080/10717544.2023.2186312
[38] E.M. Arroyo-Urea, et al. Drug Deliv. 30, 2179128 (2023). doi: 10.1080/10717544.2023.2179128
[39] K. Nienhaus, et al. Small 2301663 (2023). doi: 10.1002/smll.202301663
[40] A.E. Goode et al. Nanoscale 7, 1534 (2015). doi: 10.1039/c4nr05922k
[41] A.L. Kholkin et al. "Review of Ferroelectric Domain Imaging by Piezoresponse Force Microscopy", in "Scanning Probe Microscopy" ed. S Kalinin and A Gruverman (New York: Springer) pp 173–214. doi: 10.1007/978-0-387-28668-6_7
[42] Hruszkewycz et al. Phys. Rev. Lett. 110, 177601 (2013). doi: 10.1103/PhysRevLett.110.177601
[43] S. Kaufmann et al. New Journal of Physics 13, 055029 (2011). doi: 10.1088/1367-2630/13/5/053029
[44] M. Ahart et al. Nature 451, 545-548 (2008). doi: 10.1038/nature06459
[45] Acharya et al. Chem. Mater. 34, 9613 (2022). doi: 10.1021/acs.chemmater.2c02295
[46] U. Schroeder et al. Nat. Rev. Mater. 7, 653-659 (2022). doi: 10.1038/s41578-022-00431-2
[47] L. Rodríguez, et al. Acta Mater. 220, 117336 (2021). doi: 10.1016/j.actamat.2021.117336
[48] F. Xue et al. Phys. Rev. B 94, 220101 (2016). doi: 10.1103/PhysRevB.94.220101
[49] S.R. Bakaul et al. Advanced Materials 32, 1907036 (2019). doi: 10.1002/adma.201907036
[50] S. Bajt, et al. Light Sci. Appl. 7, 17162 (2018). doi: 10.1038/lsa.2017.162
[51] E. Nazaretski, et al. J. Synchr. Rad. 22, 336-341 (2015). doi: 10.1107/S1600577514025715

2 - User community (approximately 2 pages)

CoDI will tackle the scientific challenges of many different communities: semiconductors, catalysis, energy related materials, quantum materials, etc., see above. The CoDI core team, listed in section 7, will act as nucleation seeds for attracting and aggregating further Spanish users. If the beamline is retained, a program for broadening the academic and industrial user communities is necessary. Even if there are national research groups that will profit from day one, broadening these communities within Spain is required to fully exploit CoDI. This is acknowledged, and ALBA is already organizing a workshop in earth and planetary sciences in summer 2023.

- Industry users are expected. For instance, ptychographic techniques are already being used to image chips. Members of the CoDI core team will assist in outreaching CoDI capabilities and performances to the interested industrial users mediated by the ALBA industrial office.

In the following analysis, the discussion is centered in the Spanish community, as the relatively large portfolio of techniques at CoDI does not allow to discuss the foreign communities in the available limited space. It is worth noting that the three Spanish researchers leading this proposal, who are currently working in key European large infrastructures (European XFEL, University of Lund - MAX IV, and PSI-SLS) see section 7, are in a privileged position to witness and contribute to enlarging our community. They will also help to establish connections and collaborations between experienced Spanish researchers and interested (future) users. The next paragraphs highlight the targeted Spanish communities that will highly benefit from CoDI performances. The researchers that will initially lead the efforts to enlarge the communities are also listed. It is expected that other colleagues will join this endeavor.

♦ Semiconductors. Lucia Aballe (ALBA) and Jose Antonio Garrido (ICN2-Barcelona).

There is a wealth of Spanish institutions and companies involved in microelectronics research and innovation which will benefit from non-destructive 3D/4D imaging with nanometer resolution and element specificity. Just in the nearby area, one finds the following interested partners: Centro Nacional de Microelectrónica CNM-CMB, Catalan Institute of Nanoscience and Nanotechnology, ICN2, UAB, IFAE and ICFO. Other potential CoDI users are the high-tech start-ups that will access the services of InnoFab such as INBRAIN Neuroelectronics (neuroelectronic therapies based on graphene), Qilimanjaro Quantum Tech (full stack system of quantum hardware and software), or Qurv Technologies (wide-spectrum image sensor technologies). Moreover, many other organizations located all over Spain will benefit from CoDI outstanding performances.

♦ Catalysis. José Solla Gullón (Universidad de Alicante) and Víctor A. de la Peña (IMDEA-Energia-Madrid).

There are many Spanish groups involved in different catalytic processes including those focused on environmental and energy-related technologies. We can point out some CSIC research centers: Instituto de catálisis y Petroleoquímica (Madrid); Instituto de Ciencia de Materiales de Madrid (Madrid); Instituto de Tecnología Química (Valencia), Instituto de ciencia de Materiales de Sevilla (Sevilla); Instituto de cerámica y Vidrio (Madrid); Instituto de Nanociencias y Materiales de Aragón (Zaragoza); Instituto de carboquímica (Zaragoza); Instituto del carbono (Oviedo). Moreover, many universities have strong research groups in catalysis that are too many to be listed here. Finally, there are other institutions such as CIEMAT, IMDEA-Energía, IMDEA-Nanociencia, IMDEA-materiales, CIEMAT, ICN2, ICIQ, Energygune, ICMoL and IREC. The Spanish Society of catalysis (https://www.secat.es/) has more than 500 members and it meets every two years. SECAT is the ideal tool to outreach CoDI capabilities to the full community.

♦ Quantum materials. Allan Stewart Johnson (IMDEA-Nanociencia-Madrid).

Quantum materials are a major focus in the Spanish condensed matter physics community, with important seed communities at the Donostia International Physics Center, the Instituto de Nanociencia y Materiales de Aragón, the Institut Català de Nanociència i Nanotecnologia, IMDEA-Nanociencia, the Universidad Complutense de Madrid, the Institut de Ciència de Materials de Barcelona, the IFIMAC center and the Instituto de Ciencia de Materiales Madrid, among others. One of the two major networks of the División de Física de la Materia Condensada-GEFES of the RSEF is focused on quantum material, and quantum materials were the sole focus on two consecutive biannual meetings in 2015 and 2017.

♦ Earth and Planetary sciences. Catalin Popescu (ALBA).

There are several Spanish groups involved in research projects using synchrotron radiation on Earth and Planetary materials. We can highlight among others: Institute of Space Studies of Catalunya, Institute of Space Science-CSIC, Center for Space Research-UAB, Institute of Cosmos Science-UB, Research Group in Space Science and Technologies-UPC), Institute of Geoscience Barcelona-CSIC (for instance, Jesus Martinez Frias is involved in Nasa Mars mission) and University of Basque Country (Juan Manuel Madariaga in charge of Spanish network of Mars exploration).

♦ Geochemical dissolution and precipitation processes. Irene Calvo (Universidad de Zaragoza) and Miguel A.G. Aranda (Universidad de Málaga).

Firstly, there is a large Spanish community working on imaging the hydration of cements. However, so far most works are related to classical electron microscopies. The activities are mainly based at the Instituto Eduardo Torroja (CSIC-Madrid). This CSIC-institute is fully devoted to construction materials. Moreover, there are other research groups for instance at UPC and UPV. The group at University of Malaga will outreach CoDI capabilities to this community. Secondly, the mineralogical community in Spain is larger. The Spanish mineralogical society was founded in 1975 and it has 250 active members. They meet annually and if CoDI is retained, it is planned to outreach CoDI capabilities at their meetings. The research group at Universidad de Zaragoza will lead this endeavor.

♦ Magnetic Nanoparticles in Biological systems. Jesus Blanco (Universidad de Oviedo).

The Spanish Association on Magnetism (CEMAG, https://www.cemag.es/) brings together members of the national scientific and engineering communities who are interested in in all aspects of fundamental and applied magnetism. Topics range from fundamental magnetism to advances in magnetic recording, emerging applications in energy and power technologies, and magnetic nanoparticles and biomagnetism, to name a few. The association has around 350 members, including many international highly-reputed scientists. CoDI support team has members of CEMAG and will push to attract more close this community.

♦ Complex oxide thin films. Carlos Frontera (ICMAB-CSIC).

There are many research groups working in thin films, oxide and related materials, with a strong diffraction background. These groups will immediately benefit from the nano-diffraction and nano-XRF capabilities. With the required training, some will also benefit from the advanced imaging performances. Within the nearby CSIC-institute ICMAB, we can highlight: -Superconducting materials and Large Scale Nanostructures; -Laboratory of Multifunctional Thin Film and Complex Structures; and -Advanced Characterization and Nanostructured Materials. Moreover, there are also research groups at ICN2 and at UAB. It is not possible to mention all groups working in this subject at the Materials Institutes of CSIC and those located at Universities. Our strategy is to profit from the Spanish Group of Crystallography and Crystal Growth-GE3C (https://ge3c.rseq.org/) in order to show CoDI capabilities and performances. This group meets annually and it will be a natural place to frame not only the required outreach, but also to address the training of the interested researchers through the ‘school’ program.

3 - Beamline description detailing the following main components (including key performance parameter for each chapter) (approximately 15 pages)

The CoDI beamline aims to deliver an optimized nano-focused beam at the sample position with a high flux and a large transversal coherence. For that, a long distance from the source to the sample position and a high-performance optical system is required. Here we demonstrate the feasibility of designing and constructing the CoDI beamline using state-of-the-art components and technology that currently exists. With this goal, we will evaluate the main components and performance of the nano-focused X-ray beamline. Nevertheless, this design will be optimized during the design phase of the beamline, taking into account the latest developments and technology at that moment, since we expect the current technology to quickly evolve to provide better performance systems and equipment.

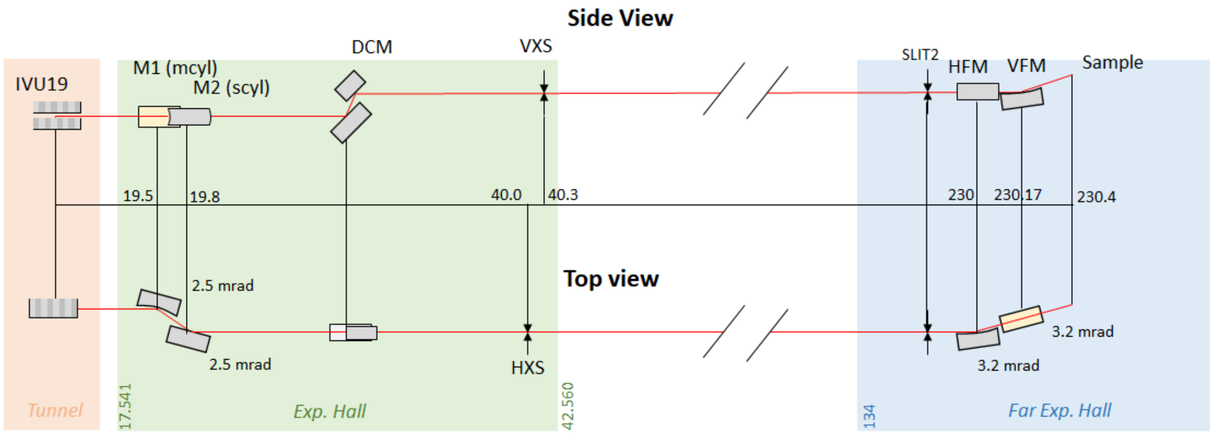

Figure 8. Optical layout of CoDI beamline containing the principal optical elements and their position in meters with respect to the source. The tunnel, the experimental hall and the far experimental hall are also identified.

Fig. 8 depicts the overview of the preliminary design of CoDI beamline, which contains the principal elements and their distance with respect to the source are depicted. Briefly, the beamline will consist of an *in vacuum* undulator ("IVU19") that will be the photon source. Then, after the front-end, the mirrors M1 and M2 will focus the divergent beam into the secondary source (VXS, HXS). In the path, the X-ray beam will be monochromatized by a Si(111) or a Si (311) double crystal monochromators (DCM), whose selection will depend on the high flux or high energy resolution respectively. Moreover, a multilayer system will be also available to increase the high photon flux at expense of the energy resolution, as some photon consuming/time resolution experiments require. In the far experimental hall, the X-ray beam will be cleaned by a secondary slit system (slit2) and focused with a set of moveable KB mirrors (HFM, VFM) that can also be moved out of the X-ray beam path to allow other optical setups to interact with the beam, as the proposed MLLs system for further nano-focus the beam for very high-resolution imaging. Surrounding the sample will be the sample positioning system and the sample environment to perform *ex situ, in situ* or *in operando* experiments. Finally, a set of (area) detectors that will record the scattered and/or fluorescence radiation will be installed, highlighting the long sample to detector distance in the forward direction up to 20 m to ensure enough spatial resolution to resolve the recorded information.

Below, a more detailed description of these and other components that could form part of the CoDI beamline are presented:

3.1. Photon source.

A state-of-the-art planar undulator has been selected as a photon source. The undulator will be optimized to deliver high spectral brightness, tunability with tapering capabilities in the working range between 10 and 30 keV, being possible to extend this range on demand, especially towards lower energies. Based on a preliminary design, an in vacuum undulator with a period of 19 mm will fulfill the requirements (Fig. 9). The fundamental energy of this undulator (1st harmonic) has been calculated at 1.297 keV, meaning that a high flux of lower energy (< 10 keV) photons could also be delivered. As an illustration of its performance, at 250 mA of current in the storage ring, the flux at 20 keV will be 10^{14} ph/s/0.1%BW. Horizontal linear polarization will govern the polarization of the produced X-ray beam, but in the case of polarization analysis, thin crystal phase plates could be easily installed to tune the polarization of the X-ray beam.

The maximum power of the IVU19 has been calculated to be 4 kW at 3 keV and 250 mA. This power load will require the use of common strategies to ensure a correct power management, e.g. limitation of the accepted aperture, use of cooled water masks, distributing the power between several elements. This is a common practice at ALBA, as described here below in the beam transport section.

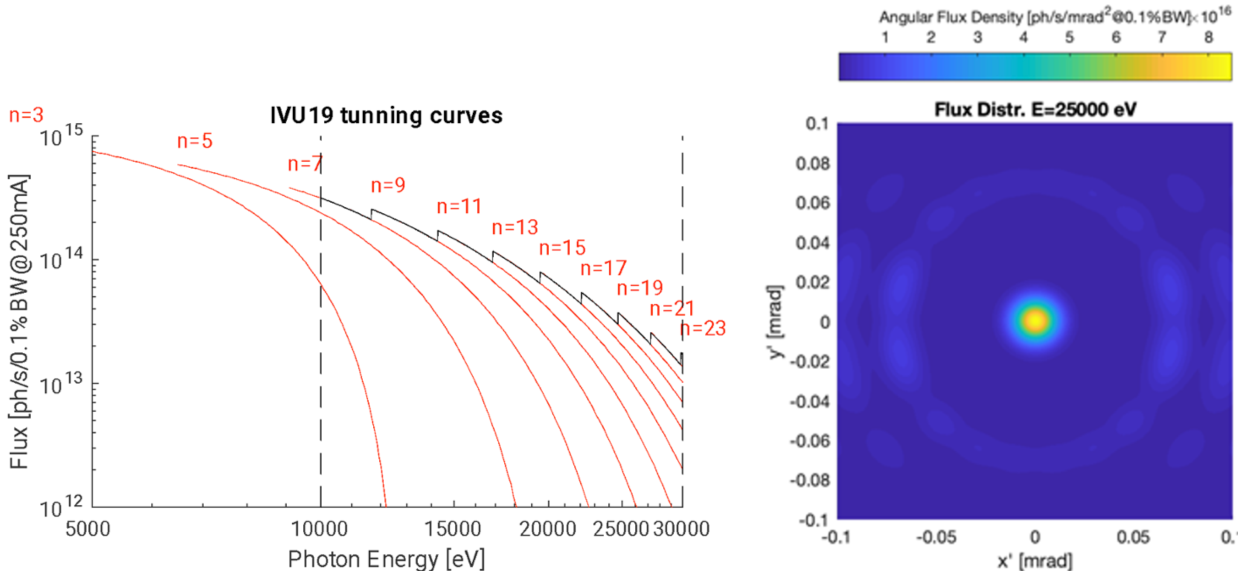

Figure 9. Left: Tuning curves for the integrated flux at 250 mA of the IVU19 proposed, identifying in between the dashed lines the optimal working energy range of CoDI. The minimum magnetic gap of the IVU19 is 5.2 mm, which corresponds to a deflection parameter of K = 2.14. Right: Angular flux distribution at 25 keV (19th harmonic), with a peak flux density of 8.51·10^{16} ph/s/mrad2/0.1%BW and a vertical and horizontal divergence of 23.87 x 18.66 μrad^2 (FWHM).

3.2. Beam transport.

- **Front End**

The front end will follow ALBA standards for the front end for undulator sources. It will consist of a set of masks, an X-ray beam positioning monitor to detect changes on the beam position, a photon shutter and a trigger unit with a fast-acting valve to protect the and isolate the vacuum of the beamline and the storage ring. The exact design of the masks will be optimized using finite element calculations for the deformations and distortions induced by the high-power X-ray beam at the different surfaces of the optical components.

- **Pre-focusing mirrors**

The first optical element will be a set of two horizontal offset focusing mirrors: A meridional (M1, 400 x 4 mm^2) and a sagittal (M2, 400 x 3 mm^2) cylindrical mirrors with fixed radius. They will be placed in the same vacuum chamber with a common vacuum platform to have an optimal stability. Both mirrors will be coated with an Ir layer with a final slope error < 0.2 mrad. The working incident angle of the X-ray beam will be 2.5 mrad, deflecting the beam outboard and inboard respectively.

These mirrors will serve different purposes:

- **Focusing**: The X-ray beam will be focused in the secondary source located ca. 40 m downstream the source, the mirrors M1 and M2 will be used for the horizontal and vertical focus, respectively.
- **Power absorption**: The first mirror M1 will absorb a fraction of the power of the white beam. To hold this power load, M1 will be side cooled.
- Harmonic **suppression**: The high energies harmonics produced by the IVU19 insertion device will be rejected in the first mirror.

- **Monochromator**

CoDI beamline has been optimized to work within an energy range of **10-30 keV** depending on the specific scientific case, being also possible to produce lower and higher energy X-ray beam at expense of the beam size and photon flux respectively. This possibility would be of interest for accessing spectroscopic experiments of transition metals and/or to investigate larger samples that require higher penetration depth.

With this aim, the white beam produced by the insertion device has to be monochromatized to deliver a monochromatic X-ray beam with a minimum energy bandwidth and maximum photon flux. The preliminary design of CoDI require two types of systems to monochromate the X-ray beam: i) a couple of Si **double crystal monochromators** (DCM) with orientation **Si(111) and Si (311)** with a minimum resolution of $\Delta\lambda/\lambda = 6\cdot10^{-4}$ and $5\cdot10^{-5}$ respectively at 20 keV; and ii) a **double multilayer (ML)** that will partially cover one pair of crystals, with minimum resolution $\Delta\lambda/\lambda = 10^{-2}$. The resolution will depend on the energy selected, but this combination will fulfill all the requirements for delivering a high-performance X-ray beam. In fact, the double pair of Si monochromators has been considered to cover the full required energy range with the possibility of being optimized for flux (Si (111)) or energy resolution (Si (311)). Complementarily, the multilayer solution has been considered to increase the photon flux by one order of magnitude at the expense of decreasing the energy resolution. This set of monochromators/ multilayer will be critical for experiments that require high energy resolution or that are highly photon consuming, e.g. time resolution experiments, but also perhaps some imaging experiments with holo-tomography and ptychography. The design and the proposed mechanics will enable the possibility of performing energy scans near an absorption edge at moderate speeds (1eV/s) and/or to perform a combined coherent experimental technique while also retrieving 3D elemental information of the sample volume.

Both systems (*i.e.* monochromators and multilayer) will be placed in the same vacuum chamber and supported by the same high precision mechanics, enabling the possibility of a fast crystal pair exchange when required. The option of placing the multilayer covering part of one of the crystals is an optimal solution already implemented at the FaXToR beamline that allows selecting the Si crystal or the ML in an easy and efficient way. Moreover, the set of monochromators will be designed to have a fixed vertical exit position, ensuring a constant X-ray beam vertical position independent of the energy employed. Because of the high X-ray beam power, the monochromators will be cryocooled with liquid N_2, which is a common practice at ALBA for the beamlines whose X-ray beam is produced by an insertion device.

- ## Secondary source

The pre-focusing mirror will image the real source at a focus located at around 40 m from the source. In this position, a set of vertical and horizontal slits will define a secondary source. The aperture of the slits will be defined as a compromise between the flux and coherent fraction of the beam needed for each particular experiment. This will result in the possibility to adapt the flux vs focal-spot size in the experimental endstation before the final focusing optics. Closing the secondary source will reduce the beam spot size at the sample position but it will also determine the coherent flux fraction of the X-ray beam at the sample position. In Fig. 10 the coherent fraction for the different energies and apertures of the secondary source are presented. As expected, a smaller aperture entails a larger coherent fraction, being less sensitive to variations in energy. For small apertures (e.g. 2x3 μm^2) a highly coherent beam (> 95%) has been calculated for all the working energy range of the CoDI beamline.

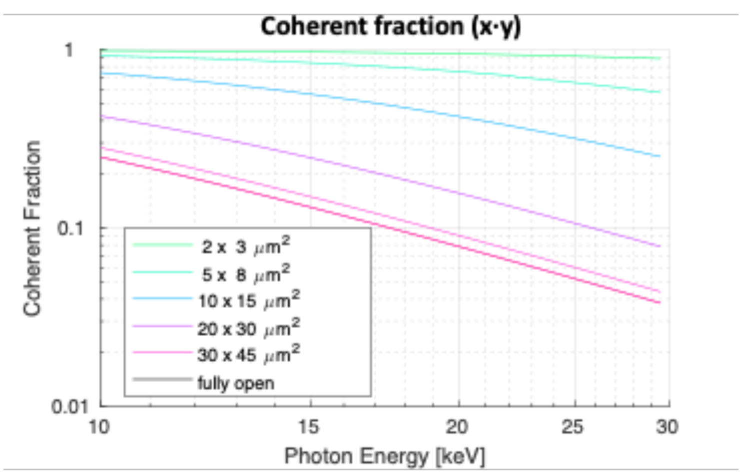

Figure 10. Calculated coherent fraction of the photon beam for the different energies depending on the aperture of the secondary source. Highly coherence is achieved when the aperture of the secondary source is reduced.

Furthermore, using the secondary source will benefit the X-ray beam stability at CoDI’s end station, since the secondary source will **filter upstream vibrations of the photon beam**. This is critical for a high performance nano-focused beamline.

- **Focusing optics**

To deliver an optimal X-ray photon beam along of the full working energy range of CoDI beamline (*i.e.* 10-30 keV) the preliminary design has considered the use of two pairs of KB mirrors that have been optimized to work at 15 and 25 keV: the first pair of mirrors (optimized for 15 keV) will have a Rh coating while the second pair (optimized for 25 keV) will have an Ir coating to maximize the reflectivity, being the working incident angle 3.8 and 2.8 mrad respectively. As illustration of the acceptance of the KB mirrors, preliminary calculations resulted in an acceptance of 570 µm and 336 µm in the horizontal (HFM) and vertical (VFM) directions respectively at 20 keV. Concerning the performance to produce a nanobeam, for example, at 20 keV a diffracted limited beam of 32 x 32 nm^2 (FWHM) will be produced with a divergence of 3.2 mrad in both directions (Fig. 11). It is worth mentioning that the diffraction limited and highly coherent X-ray beam is achieved by closing the SSA, but if required, larger beams can be achieved by opening the SSA, which will also increase the photon flux in the sample position (at expense of the coherent fraction). This will enable the possibility of having a larger focal spot that could be of interest for some cases using, among others, the diffraction and diffraction imaging techniques.

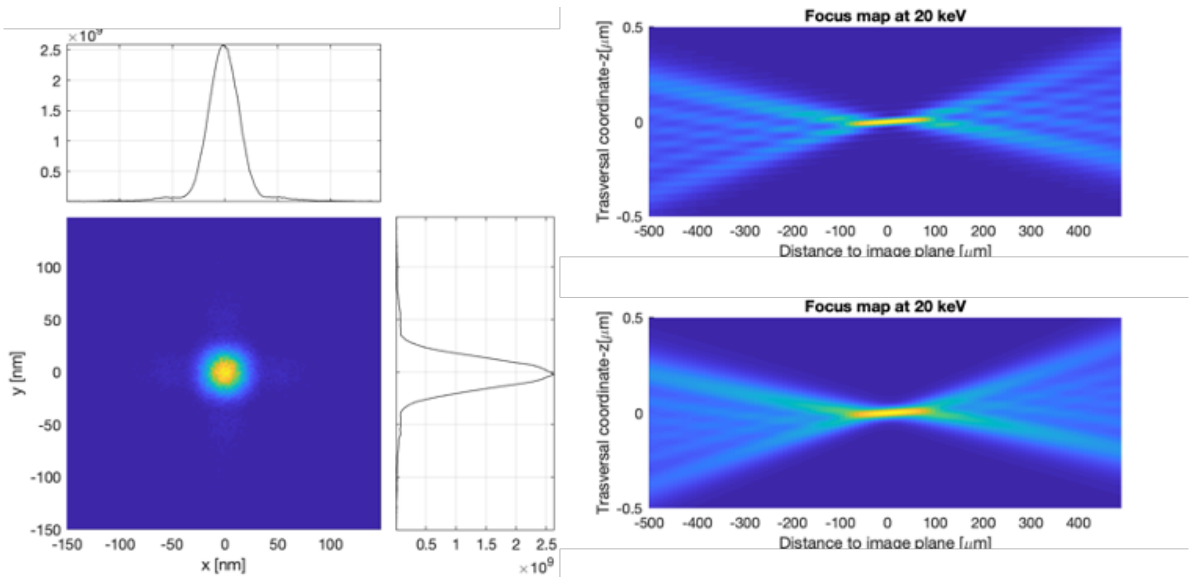

Figure 11. Simulation of the 20 keV X-ray focused beam at the sample interaction point with a resulting diffraction limited X-ray beam of 32 x 32 nm^2 (FWHM) (left) and beam propagation for a highly coherent diffraction-limited beam (right, top) and for a high flux beam (right, bottom) achieved by closing or fully opening the secondary source aperture respectively.

This preliminary design results in a working distance from the last mirror to the sample (focal point) of 150 mm, which will enable the possibility of placing dedicated sample environments for *in situ* and/or *in operando* experiments, a key point of the CoDI beamline. Fig 12 depicts the preliminary design of these two pairs of KB mirrors located at 230 m from the source. Both sets of mirrors will be facing each other inside the same vacuum chamber with its own mechanics for alignment and positioning, and they will also have a common vacuum system. Moreover, in addition to the internal movement of the mirrors to be placed in or out of the X-ray beam, the complete vessel (*i.e.* the complete chamber containing the mirrors and the mechanics) can be removed out of the beam using a motorized system. In this way, room for installing alternative optical/mechanical systems and/or specific sample environments will be possible.

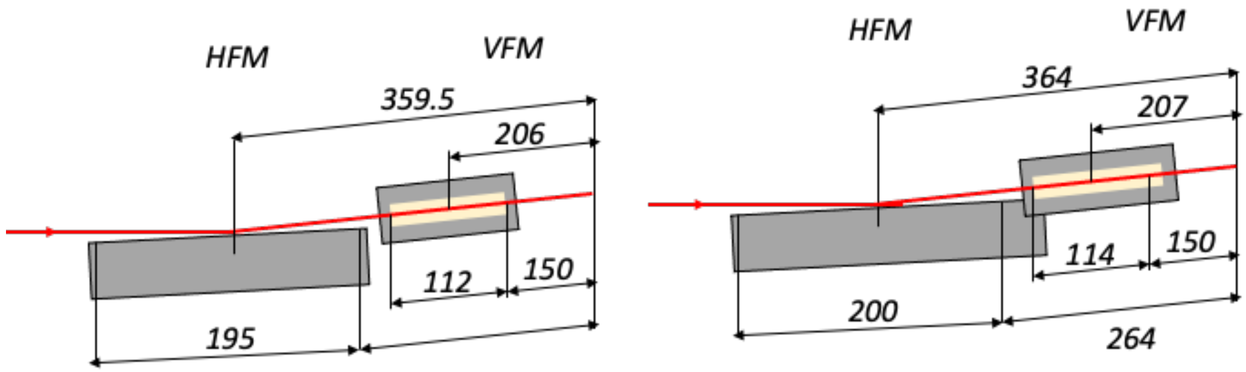

Figure 12. Dimensions of the KB mirror systems for low (left) and high (right) energy ranges optimized at 15 and 25 keV respectively. The mirrors will be coated with Rh [Ir], with working incident angle of 3.8 [2.8] mrad for the low [high] working energies ranges.

Aiming to push the singularity and performance of CoDI beamline, a second setup based in MLLs is proposed in addition to the KB mirrors. With this solution, a beam of 6 x 6 nm^2 (FWHM) will be obtained at the sample position, pushing the limits of the current state-of-the-art nano-focused beamlines. With this setup, a working distance between the MLLs and the sample position will be ca. 10mm, but we expect the current technology to quickly evolve, improving the currently the limitations of the MLLs fabrication methodologies, and hence, allowing to significantly increase the working distance. This setup will be positioned over its own positioning system (*e.g.* hexapod) to align the MLLs along the beam path near the sample position, ensuring a correct alignment of the MLLs and that the sample can be scanned in the defined focal point.

Both focusing systems (*i.e.* KB mirrors and MLLs) will be easily exchangeable with a high precision and reproducible motorized system, that briefly will displace the KBs out from the beam path to let the full X-ray beam to interact with the MLLs to produce the nano-focused beam.

- ## Diagnostic system

The diagnostic system is a key point of the beamline to **deliver a high-quality beam**. It facilitates the commissioning and configuration of the beamline for the different experiments that will take place. For that, the diagnostic system requires different elements with different functions along the beamline. Here, some of (but not limited to) the basic components of the diagnostic system that could be installed are described:

- Beam screen monitor after the pre-focusing mirrors: The X-ray beam shape will be monitored prior to the monochromator to ensure a correct beam shape of the white beam. Because of the high power, attenuation of the direct beam or active cooling would be required.
- Transmissive photodiode: Located in the same vacuum vessel of the monochromator, the positioning photodiode will help to optimize the monochromator alignment.
- Positioning system: In order to ensure a fix the entrance position of the X-ray beam into the secondary source aperture, a nano-positioning system will be placed in front of the secondary source. The system will act in a high frequency closed loop state to correct the beam position by acting on the second crystal of the monochromator.
- Beam screen monitor: Located after the secondary source, it will serve to monitor the X-ray beam shape at the exit of the near experimental hall (current ALBA slab).
- Positioning system: The first element on the far experimental hall (new building) will be a positioning system that will help to monitor drifts on the X-ray beam after traveling from the near to the far experimental hall.
- Beam screen monitor: To monitor the demagnified X-ray beam shape in the far experimental hall, a beam screen monitor will be placed in the experimental hutch. It will also be located before any of the focusing elements (*e.g.* KBs*,* MLLs) to ensure the correct beam shape before the final focusing stage.

- X-ray wavefront sensor: In order to measure the optical wavefront, a sensor to describe the X-ray beam shape and phase will be installed, profiting the long camera length. An on-line reference system will be installed with the possibility of inserting or removing it from the X-ray beam path to investigate the possible wavefront distortion and take actions to minimize the possible optical aberrations.
- Laser tracing: A visible-light and low power laser will be required to visualize the X-ray beam path from the optical hutch until the detector (straight line). This will help during the commissioning to visualize and approximate the X-ray beam path through the different elements (*e.g.* vacuum line, slits, sample environment, flight tube).

- ### Slits system

Different sets of masks/slits systems will be installed in CoDI in order to deliver the appropriate high-quality X-ray beam:

- Fixed masks: Water cooled fixed mask located after the front end to absorb part of the white beam power.
- First slits: After the monochromator, there will be a set of slits to clean the X-ray beam that travels towards the secondary source.
- Secondary source aperture: The secondary source will define the X-ray beam size that will be accepted by the focusing system, that at the end defines the beam size and coherent properties at the sample position.
- Second slits: Located at the beginning of the far experimental hall, they will serve to clean the X-ray beam generated by the secondary source.
- Guard slits: Anti-scatter slits systems to ensure a high-quality beam.
- Fast shutter: Required to minimize beam exposure if data collection is not demanded, it will block the X-ray beam and it will only open the path to the X-rays when the data need to be acquired. The action time should be in the order/below of the millisecond, and it should be synchronized with the beamline and the full acquisition system.

- ### Attenuation system

Beam damage on the sample has to be minimized. For that, and due to the high power of the X-ray beam, a set of fast acting filters will be installed after the monochromator to reduce the photon flux that will arrive to the sample. This will also help to perform commissioning tasks without the full beam intensity. The set of filters will consist of single crystals of Ge, Si and CVD diamond to conserve the coherent properties

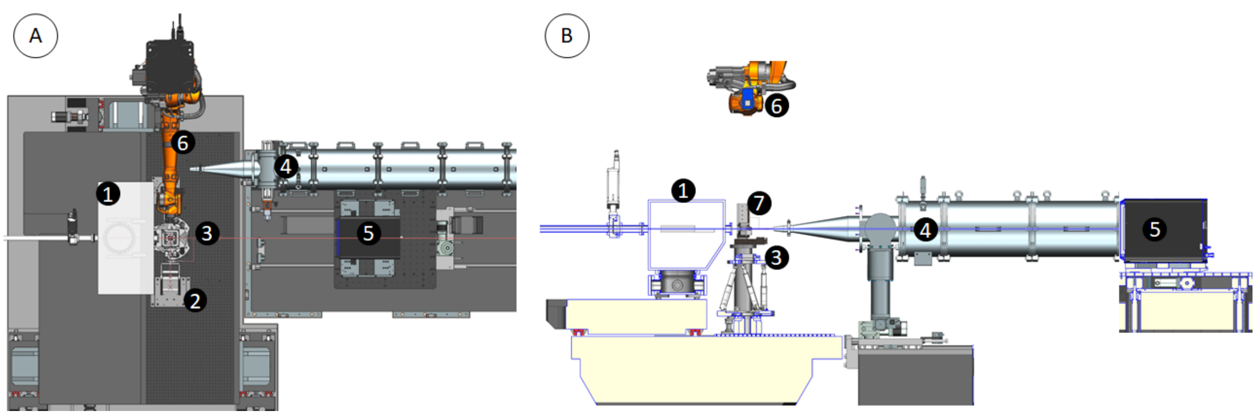

Figure 13. Top view (A) and side view (B) of CoDI end station where different elements are identified: 1- KB mirrors vessel with 2 pairs of KB mirrors and free path for the X-ray beam; 2 - MLLs positioning system (removed from B for clarity); 3- Sample positioning system composed by a a rotation goniometer, an hexapod and high-precision linear and rotation stages; 4- Modular flight tube that can be retracted from the X-ray path (A) or be inserted (B), and it can be also extended up to 20 m, allowing the area detector to reach the sample position and to record the scattering signal at 20 m minimizing the air scattering and absorption; 5- Area detector positioned a movable table with X and Z movements that could be also inserted inside the flight tube for in vacuo experiments; 6- Robot supporting the small pixel size detector; 7- Fluorescence detector supported and pointing to the sample. Some motors and components are not shown in the image for clarity. The X-ray beam is the horizontal red line traveling from left to right of the image.

of the wavefront. Different thicknesses will be possible to be combined using pneumatic actuators, enabling the possibility to attenuate the beam in different proportions.

3.3. End station

The CoDI beamline will be a state-of-the-art versatile nano-focus beamline that will allow to perform different kinds of experiments and that will be open for new challenges in the future. In fact, the design of the CoDI end station will follow the experience of similar beamlines at other facilities, pushing the boundaries of the available resources and technology.

CoDI endstation will be formed by four different main parts: granite table, focusing system, sample environment and detection system; each of them subdivided in the different components. CoDI will be highlighted by its versatility, since it will be capable of hosting different optical elements (*e.g.* KB mirrors, MLLs or other future systems) and sample positioning (*e.g.* scanning stages, diffraction setups), sample environment equipment (*e.g.* temperature control, laser, high pressure, gas atmospheres, or any user system) that will be easily exchangeable. Fig. 13 depicts some elements composing the end station, where the essential elements as the optical focusing system, the sample positioning stages and the detectors are shown.

To demonstrate the feasibility of easily exchanging the KBs and the MLLs focusing systems, Fig.14 shows an image where the main components in the MLLs configuration with the KBs out of the X-ray beam path are presented. As it can be observed, just by moving the KB mirrors inside the chamber out of the beam path using the internal high-precision motors, the micrometric X-ray beam passes through the chamber to find the MLLs located after the KB mirrors chamber. The MLLs will have its own sample positioning environment that will allow their orientation with respect to the X-ray beam. A general view of the end station (Fig. 14, C) is presented to put in perspective the sample positioning system with respect to the total length of the end station.

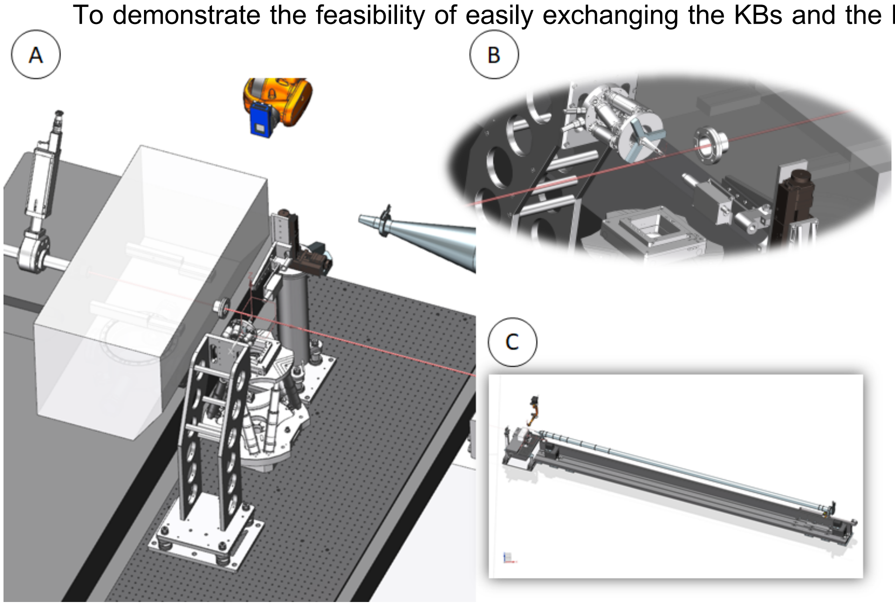

Figure 14. Close overview of the experimental end station, with the MLLs configuration (A), where the X-ray beam passes through the KB mirrors vessel to be focussed with the MLLs system (with its own positioning system) with a working distance < 10mm from the sample position (sample holder not shown for clarity) (B). General view of the experimental end station, showing the length of the flight tube and the two extreme possible detector positions (C).

Here the main components forming part of the end station are detailed, in order to give an overview of the different components and their purpose by categories:

- ### Sample positioning system

Working with a nanometric X-ray beam and micrometric samples require the use of high precision and reliable motors. Therefore, the setup proposed for CoDI will serve, first, to position the sample into the X-ray beam, and second, to scan the sample in the different spatial and angular directions required for the experiment. The versatility of the CoDI beamline demands adequate sample positioning systems that could be different for the different available techniques. Moreover, room for future improvements/setups for specific user cases (including the optics) could also be accommodated in the experimental hutch. For that, the essential sample positioning system will be composed by a modular system with different elements that can be adapted to the specific porpouse:

- A goniometer rotation stage (ω) will be located on a granite base, covering +/- 180º rotation. This will enable the possibility of rotating the sample with the X-ray beam and help in both 3D scanning and diffraction experiments.
- Hexapod: This will be placed on the goniometer. With the 6 degrees of freedom, it will be used to move the sample into the X-ray beam that will be perpendicular to the ω rotation axis. Thanks to the possibility of defining a virtual rotation point, the sample can be located at different spatial positions over the stage. Over the hexapod, different scanning stages can be mounted depending on the experiment to be performed.
- 2D/3D scanning: The sample will be mounted on piezo-scanning stages located on the hexapod that will allow scanning the sample in the three spatial directions (X, Y, Z). The scanning range of this stage will be identical in all directions, 100 µm.
- Surface diffraction: On top of the hexapod, a high precision diffraction setup could be mounted to allow χ translation and φ tilts and all the required movements to perform surface diffraction experiments with nanometric resolution. In this case the piezo scanning stages will be located to allow the location of the samples in the center of rotation of this 3-circle system (ω, χ and φ).
- Tele-ptychography: a pinhole analyzer will be located few millimeters away from the sample in its own scanning piezo stage, this stage will be mounted in a set of coarse motors that will allow to center it to the beam and also rotated around the vertical center of rotation of the sample goniometer for diffraction experiments.

In order to increase stability against potential vibrations, the optics and sample positioning system will be placed over a large granite block. This granite table will be large enough to allocate the defined optics (*i.e.* KB mirrors & MLLs) and sample positioning and environment hardware. For example, in the case of the MLLs, a second positioning system (*e.g.* small hexapod) will be installed, allowing enough degrees of freedom to position the MLLs along the X-ray beam axis and near the sample position. Moreover, this granite table will permit the placement of future experimental chambers or systems for specific scientific cases or for future beamline improvements. Nevertheless, knowing the exact position of the sample with respect to the focusing system is critical, especially for the imaging experiments where data reconstruction relies on the fix illumination with the X-ray beam. To tackle this issue and improve the data quality of CoDI and the efficiency of the beamline, an interferometric system with active correction between the sample and the focusing system (*i.e.* MLLs or KBs) will be also installed as a part of the sample positioning system.

- ### Flight tube

The high performance of CoDI relies, among other things, on a large sample-to-detector distance in forward direction from the sample position up to 20 m to better resolve the collected data for the different coherence diffraction and imaging experiments that CoDI will host. To prevent air scattering and absorption, a flight tube in primary vacuum (ca. 10^{-3} mbar) will be installed. At the entrance and exit parts of the flight tube, a highly X-ray transparent window will be installed. The acceptance of the entrance and exiting windows will be enough to ensure a full detector sensitive area coverage (ca. 250 x 250 mm^2), being possible to adapt the entrance system for larger or smaller windows when required. The flight tube will be also modular as in many of the SAXS beamlines worldwide, allowing shortening or enlarging the distance by removing or including more parts in the tube. This will also enable the possibility of dividing the flight tube in parts where the area detector can be intersected thanks to the detector positioning system to place it at the desired position. The flight tube system will be also motorized to properly align the system horizontal axis with respect to the beam path, avoiding physical limitations to position the sample and the appearance of dark regions on the detector because of the shadowing of the flight tube components. Since for some experiments the X-ray detector must be *in vacuo* to ensure high data quality, the flight tube will be also compatible with an *in vacuum* detector installation.

- ### Beamstop system

A set of beamstops will be designed to block the direct beam when needed prior to the X-ray detector to avoid system damage. For that, *in vacuum* and *in air* beamstops placed inside and outside the flight tube respectively will be available. These beamstops will be motorized, being possible to position them in the X-ray beam path independently of the sample and detector positions. This approach is the typical solution of the scattering/diffraction beamlines.

- ## Detectors

CoDI will perform different kinds of experiments that require the use of several detectors that could be used simultaneously for some of the experiments. All detectors will be optimized for (but not limited to) the main energy range of the beamline, *i.e.* 10-30 keV:

- Forward direction: single photon counting pixel detector with a large sensitive area (*e.g.* 225 x 225 mm^2) and small pixel size (≤ 80 x 80 μm^2) based on CdTe/GaAs technologies for the high energy. It will be located in the forward direction with a minimum and maximum sample-to-detector distance of 10 cm and 20 m respectively, being compatible with vacuum to enable the possibility of inserting it inside the flight tube. It will be a fast detector (*e.g.* frame rate > 500 Hz) that will enable the possibility of measuring relative fast kinetics during *in situ* or *in operando* experiments. This detector will be combined with the flight tube to position the detector at the desired sample distance for resolving the scientific case of interest.
- Diffraction: another single photon counting pixel detector with smaller active area and pixel size (< 60 x 60 μm^2) will be used for recording diffraction peaks. Because of the small detector size and weight, it will be positioned on a robot arm that will allow it to freely position the detector around the sample, allowing the possibility of scanning ¼ of the Ewald sphere or more. The use of the robot will enable changing the rotation point of the detector depending on the sample environment and scan the reciprocal space following the Ewald sphere, that together with the sample positioning system, will enable the possibility of scanning the Ewald sphere.
- Fluorescence: A high sensitivity X-ray fluorescence detector will be positioned perpendicular to the sample and X-ray beam axis to record the fluorescence signal from the sample, enabling the possibility of performing elemental and compositional 2D/3D analysis. A 5-30 keV. Si-PIN diode based with a Si thickness of 500 µm and an energy resolution 139 eV FWHM can be considered as the first solution with limitations at high energies that could require a dedicated XRF detector.

The single or combined use of the detector will be easily configured via the control system, allowing to perform acquisition with different frame rates for the different detector but being possible to correlate in time the different data recorded from the different detectors at different frame rates. Moreover, metadata from different devices and systems of the beamline will be correlated with the images in real time.

- ## Sample environments:

Based on the scientific and societal challenges that CoDI aims to tackle, different types of systems for a variety of experiments are envisioned as sample environments:

- Temperature control: a temperature control between 80-500 K with a cryostream system.
- Vacuum chamber: The installation of a vacuum chamber will depend on the kind of experiments and could be coupled to any of the other sample environment systems, e.g. air sensitive samples, gas exposure, etc.
- Gas exposure: among others, electro-catalysis *in situ* experiments will be a key point of this beamline, and therefore, sample exposure to a gas is required. For that, a gas control and exhaust system would also be needed.
- Laser system: to support the study of new quantum materials and energy materials during *in situ* and *operando* conditions, a laser system would be required at the end-station. The laser will work with fs pulses and will be triggered together with the main clock of the accelerator. This will allow the study of temporal processes from the sub-ns to the ms time scales.
- Devices: Different devices dedicated for the different scientific cases will be available. As illustration, for the microelectronics case, multicontact systems, high frequency signals generators and readers, etc. will be available; also for electrochemistry: liquid flow cells, potentiostats, etc. These devices will be available for all users at the beamline.

The key point of CoDI will be the flexibility to accommodate new and user systems in the sample position, since the relatively large spacing around from the last KB mirror (*i.e.* 150 mm) will allow the possibility of designing systems that could serve for specific types of experiments. Moreover, CoDI will also enable the possibility of including state-of-the-art systems that would contain its own focusing optics and/or sample environment combined in a single chamber that could be positioned in the experimental hutch. This successful approach has been demonstrated by leading beamlines as cSAXS (SLS), where they couple a chamber containing the optical, positioning and environment systems to the beamline to perform specific experiments that push the boundaries of the research performed.

- **Space required around sample**

The sample environment will be a flexible space that can accommodate a variety of positioning systems, chambers, devices, etc. to perform *in situ* and *operando* experiments. These kinds of experiments will be mainly performed using the KB mirror focusing system, which has been designed to have a working distance of 150 mm between the edge of the last focusing KB mirror and the focal point. The MLLs focusing system is limited because of the short working distance of ca. 10 mm, but we expect this technology to quickly evolve, enabling the possibility of performing new types of *in situ* and/or *operando* experiments. Therefore, around the sample we require a free radius of 150 mm, where the positioning system, the sample and any other related device (e.g. temperature, gas exposure, electrical contacts, vacuum chamber…) can be included.

- **Optical microscopes**

Two high resolution microscopes, one on axis and a second azimuthal (vertical axis), are required for the positioning of the sample. Several other cameras may be used for monitoring and commissioning of optical elements or the center of rotation of the goniometer.

- **Cooling system**

All the systems will be designed to hold the high thermal load produced by the highly brilliant X-ray beam, being possible the implementation of active cooling in some elements (*e.g.* fast shutter, beam stop). A detailed calculation will be done during the design phase.

- **Thermal insulation**

The CoDI beamline will require high X-ray beam stability and high reproducible precise moments to achieve the high-resolution imaging of the samples. Therefore, thermal stability around both the sample and the focusing system is a technical requirement that must be fulfilled. Due to the long distance between sample and detector, and in order to increase the thermal stability (≤ ± 0.2 ºC) a thermal “wall“ will be installed dividing the experimental hutch in two parts, minimizing the impact of thermal variations in the sample environment. This wall will be located near the sample position to minimize the air volume that requires a temperature control with high precision. The modular “wall” would allow to move the flight tube, the detector and other components from the highly controlled area to the standard-conditions part of the experimental hutch.

- **Specifications of beamline control system.**

The beamline will be fully compatible and integrated with ALBA standards, *i.e.* “Tango Controls”, which is a toolkit for connecting hardware and software together, and “Sardana”, which is devoted to the Supervision, Control and Data Acquisition (SCADA) in scientific installations. Data acquisition will rely on an efficient hardware synchronization between optical elements, sample positioning system and detection systems. The high frame rate and high scanning frequency (ca. 1KHz) requires a high performance feedback loops, to ensure that at any moment the status and position of several elements of the beamline (including the sample position) is known with high accuracy and precision to save them as metadata and/or to take the corresponding actions based on the real time information.

Moreover, the control system requires the integration not only of the common Electronic Protection System (EPS), Personnel Protection System (PSS), optical, vacuum and mechanical components of the beamline, but also will work on the integration of different elements that will serve for the commissioning and/or experiments at the beamline, as it can be the top-view and on-axis cameras, the integration of dedicated sample environments, etc.

- **Data acquisition and management.**

Data acquisition:

Data acquisition will be synchronized via hardware trigger, collecting data from the different available detectors with a high frame rate (ideally in the range of kHz), and being complemented with metadata collected exactly at the same time that the image was collected. The importance of the adequate correlation of the metadata (e.g. sample position, intensity values, etc.) with the detector data is critical for obtaining excellent results at CoDI, since data reconstruction relies on knowing with high precision and accuracy the sample position and some beamline parameters at the same moment that the data was recorded.

Data storage:

Collected data from the different detectors will be stored preferably as a compressed file (i.e. Nexus data format), containing the raw data from the detectors and the associated metadata. Different files from the same experiment will be considered as an immutable data set, with all the information required to analyze the data. The data will require to be stored following the acquisition frequencies (ca. 1KHz), so enough temporal memory and an adequate bandwidth is necessary to prevent overload of the acquisition system. The filtered data (*i.e.* useful and compressed data) will be saved temporarily in a "hot" storage for data analysis and later transferred to a "cold" storage to release storage volume. This will require a dedicated data storage for CoDI and the use of a computing system to filter and analyze the data as fast as possible to archive the collected data into the offline system.

Data reduction and data analysis:

The CoDI beamline will follow the experience and methodology of already running beamlines. First, data collection will be stored only after verifying that adequate data collection can be achieved (*e.g.* adequate sample and X-ray beam). Second, the information will be filtered before (*e.g.* detector ROI selection, acquisition frequency) and after (*e.g.* ROI selection, binning, cropping) data collection. For that, the data will be stored in a temporary memory that after filtering and verifying the data quality, it will be transferred to ALBA "hot storage" of several PB of storage. Ideally, this decision (using a dedicated data analysis pipeline) should be taken on the fly while the experiment is running using a dedicated GPU-based computing system. Finally, the data will be available in the "hot" data storage available for the data reconstruction/analysis for some time, when it will be finally transferred to the "cold" storage system.

Because of the large volume of data collected, data transfer to the home institution of the user will be limited. Therefore, a remote data analysis server (based on GPUs and CPUs) will be available to remotely visualize and process the data. This will have an impact on the amount of data stored in the "hot" system, since once the data has been reconstructed/analyzed, the raw data will be transferred to the archiving, releasing storage volume for new acquisition or data analysis.

Thus, CoDI will first use the experience of other dedicated beamlines (*e.g.* cSAXS, NanoMax) and open reconstruction procedures for data analysis, but the main goal would be also to join the data analysis community to develop new methodologies for data analysis, pushing the boundaries of the current methodologies.

In order to be able to fully develop CoDI capabilities, not only the optics, sample environment and IT hardware have to be state-of-the-art, but the software must run smoothly and in a user-friendly manner. Therefore, enough funding and human resources have to be allocated from the very beginning to software development and adaptations/tailoring of existing algorithms. It is highlighted here that imaging reconstructions will be a responsibility of the beamline. These processes have to be robust, user-friendly and as fast as possible (on-the-fly in most cases) for being able to adapt/respond to the initial results in *in situ* and *operando* experiments. Data analysis tools can/should be provided by ALBA II but these tasks should be carried out by the users.

Data management:

As stated in the current ALBA strategic plan: "Optimizing data management is key to the success of all scientific activities at ALBA". Thus, data recorded at CoDI will follow the FAIR principals: Findable, Accessible, Interoperable and Reusable. In fact, the dataset recorded at the beamline will be integrated in ALBA Data Catalog, providing by a unique Digital Object Identifier (DOI) and will become accessible after a given period of time or by request of the main proposer to refer to the data in any publication derived from the beamtime. Therefore, thanks to the metadata and the data included in the dataset files, the required information for data analysis will be available for further analysis and verification. Data management policy for CoDI beamline will also follow the strategies defined by LEAPS (League of European Accelerator-based Photon Sources) and EOSC (European Open Science Cloud), providing to the users and the scientific community a reliable and effective tool for data management with worldwide accessibility and identification.

Identify all main components.

The CoDI beamline will be the state-of-the-art coherent diffraction and imaging beamline at ALBA synchrotron. It will be characterized by the high energy accessible range, small focused nanobeam and long sample to detector distance. For that, the main components that will form part of the beamline are:

- Pre-focusing mirrors: Vertical and horizontal focusing mirrors that will mirror the source in the secondary source.
- Two Monochromator/multilayer will be used to select the energy and narrow the Darwin width of the X-ray in the range between 10 and 30 keV. One of the Monochromators will have a coated multilayer strip to increase the photon flux for certain experiments.
- Secondary source aperture: A set of high precision slits located at the focus of the Pre-focusing mirrors, the aperture of this set of slits defines the coherent fraction used in the experiments.
- Focusing system: Two focusing systems based on KB mirrors and MLLs will be used to focus the X-ray beam. The KB mirrors will give a larger beam (sub 50x50 nm^2 FWHM) with a large working distance of 150 mm that will enable the possibility of performing *in situ* and *in operando* experiments. The MLLs will provide a beam focus ca. 6 x 6 nm^2 FWHM with a working distance of ca. 10 mm.
- Sample positioning system: A rotation goniometer, and hexapod, and a set of high precision scanning stages will serve for sample positioning and scanning. For the high precision motion, the interferometer systems will be needed to feedback the data processing and the motors for increasing the resolution of the data collected.
- Detection system: A hybrid photon counting detector located in the far field (0.2 - 20m) with small pixel size (< 80 x 80 μm^2), large active area (> 225 x 255 mm^2) and high acquisition frequency (1 kHz) will serve for the imaging and WAXS experiments. A direct detector with smaller pixel size (< 60 x 60 μm^2) located in a robot arm will be employed for experiments in diffraction geometry. Finally, a Si drift detector located near the sample will record the fluorescence signal from the sample.
- Flight tube: A flight tube of 20 m will be installed to minimize air absorption and scattering. The flight tube will be modular, enabling the possibility of installing the adequate flight tube length for the sample-detector distance of interest for the experiment. The flight tube will also accommodate the detector *in vacuo* when required for the experiments to ensure high-quality data collection.
- Computing system: Data analysis requires dedicated high performance computing for remote data storage and analysis, enabling new methodologies and procedures for data analysis, reconstruction and visualization.

Any additional resources necessary to operate the beamline (sample preparation, computing, any major safety or security concerns).

The CoDI beamline will accept a variety of scientific cases that could require different tools and systems to properly develop the research. ALBA will provide this infrastructure that will be common to other beamlines/laboratories, and that CoDI users will use for different purposes:

- Laboratory access: Users may request access to chemistry, materials science, battery, catalysis, etc. laboratories, where the common tools for sample preparation will be available. Considering that the CoDI beamline will be far from ALBA main building where the current laboratories are present, a dedicated sample preparation room near the experimental hutch in the new building would be of interest.

- Clean room: In the study of microelectronics, catalysis and batteries field, but also others, users are interested in having the preparation/fabrication laboratory near the beamline, which usually is a clean room environment. In this way, the devices/materials can be fabricated in controlled conditions, preventing modifications/contaminations from external components. For that, maintenance and cleaning of the clean room is also required.
- Thermal stability: larger efforts have to be put in place to achieve thermal stability of the beamline, especially in the sample environment area. For that, new systems, solutions and protocols have to be developed to ensure thermal stability in the beamline despite the user interaction or maintenance during an experimental period that could cause thermal drifts in the system.
- Data storage and data analysis: Because of the large amount of collected data, and the required high performance computing system for data analysis, ALBA should guarantee the accessibility of the data from outside ALBA via the internet, giving access to the computing facilities for the data analysis. Moreover, there should be accessible and fast data analysis pipelines in order to achieve a correct data analysis in the minimum time, so the storage of the data can be transferred to an offline archiving system.
- Gas system: *in situ* and *in operando* experiments may require the use of gases, as in the catalysis field. For that, a system for gas injection and the corresponding gas exhaust for toxic/flammable gases should be available.
- User safety system: Beyond the PSS for the X-rays, a safety system devoted to ensuring a safe working place is required. For instance, the use of gases, laser system, etc. requires an automatic system to control all the parameters and trigger alarms and action to protect the personnel in case of any incident. Even if the hardware has been considered within the budget of the beamline, the risk analysis, the implementation of the hardware and its maintenance has to be considered.

4 – Risk management (approximately 2 pages) Identify, classify, and mitigate (if possible) main technical risks of the project.

CoDI will be one of the first ALBA II long beamlines with nano-focus capabilities. The basic technology is currently state-of-the-art, even though this could be improved during the next years, we expect that there will still be challenges to tackle during the beamline design phase. Some of the components which are standards at ALBA (e.g. undulator, monochromator, KBs, detectors), are externally manufactured even the design is done at ALBA; other components have never been implemented before at ALBA but are currently in use in other facilities (e.g. MLLs at Hard X-ray Nanoprobe at NSLS-II). In fact, CoDI will benefit from the experience of beamlines such as cSAXS (SLS 2.0-II), NanoMAX (MAX IV), 3-ID HXN (NSLS-II), I13 (DLS), ID01 and ID16-A/B (ESRF), and P06 and P10 (Petra III) in the imaging of functional materials. Therefore, we do not expect challenges that could not be overcomed by following the internal and external experience for designing and implementing the devices and components of CoDI.

Nevertheless, there are other major risks that require a mitigation plan:

- *Beam transport: from ALBA synchrotron building to CoDI experimental hutch there will be more than 90 meters of distance to be covered with a "dark" region where no dedicated equipment can be installed because of the environmentally protected area. This implies that most probably only essential vacuum systems can be installed in this region. Moreover, the long space can cause relative movements between the ALBA and the new building slabs, that could cause relative displacements of the X-ray beam over time. To minimize the effects caused by the change of the X-ray beam trajectory, high precision X-ray beam positioning monitors are required at the end of ALBA building and at the entrance of the beamline experimental hutch building to monitor these changes and put in place corrective measures as X-ray beam steering using the focusing mirrors, correction using the second crystal of the monochromator, etc.*

- *External components delay: During the present decade, several synchrotrons will upgrade their machine from a 3rd to a 4th generation. This, together with the associated upgrade and construction of new beamlines, could cause the work overload of the few specialized companies that are able to fabricate some components required for CoDI beamline. If the CoDI beamline is retained, the design and installation of the components should be started as soon as possible to ensure that the beamline is operational together with the start of ALBA II.*

- *Far experimental hall construction: CoDI will require the construction of a new building that will contain the barite concrete-based experimental hutch. This can delay the operando start of CoDI. To minimize this, the construction in the current ALBA building can be done and commissioned up to the secondary source. Also, during the dark period, offline commissioning can be also performed, dedicating efforts to the hardware, software and data analysis pipeline.*

- *Labor force: Another significant risk is the lack of specialized persons during the design and construction phase, because it will coincide with the ALBA II upgrade, so the internal resources will be limited. This applies to most of the sections in ALBA: controls, engineering, infrastructures, etc. To mitigate this, the fabrication and installation of the components will be evaluated individually with internal resources or if it has to be externalized. Also, an appropriate action and construction plan will be developed, prioritizing tasks for the initial steps of the beamline ensuring enough resources for CoDI but also for ALBA II upgrade (machine and other beamlines).* This point has been carefully considered when defining the Gantt chart for the construction of the beamline.

- *Data storage: CoDI will produce a large volume of data because of the large area detector and the high scanning speed. This could cause the saturation of the storage server. To minimize this potential issue, a dedicated part in the budget has been planned to have a dedicated storage. Moreover, the data will be first saved for validation into a local storage, and hence, only the dataset of interest with metadata will be transferred to the main storage, similar to EuXFEL. Therefore, a data management plan will be deeply investigated to ensure the viability of the data handling and storage at ALBA II, since this issue can be also extended to other beamlines as the detector technology is evolving towards faster acquisition rates for large area detectors.*

- *Budget: The current worldwide situation is characterized by a high inflation rate that causes price increase for customs and services everywhere. Depending on when the budget for the beamline is secured, the prices here stated can significantly change. To minimize this risk, a safety factor has already been implemented in the budget for a price increase within the next couple of years, but the economic evolution is difficult to predict and to precisely know the evolution of the prices.*

5 - Budget based on main components (as defined in 3)

ITEM	Budget (k€)	ITEM	Budget (k€)
IVU19	1700	Flight tube	250
Front end	400	Sample environment (including high pressure cell)	300
Focusing Mirrors and mechanics	350	Gas system including exhaust	100
DCM: Si(111), Si(311), ML	700	Sample laser system (pump-probe & heating)	180
DCM: cryocooling system	200	Radiation shielding (lead OH & concrete EH)	1500
Slits system (including SSA)	80	Control hutch	70
Diagnostics	300	Mechanical supports + crane (50 k€)	120
Photon Shutter	40	Backbone hardware	120
Attenuators	20	Vacuum standard items: FE + ID + OH	450
KB mirrors (2 pairs) + mechanics + support	680	Vacuum standard items: long pipe	150
MLL + mechanics (including interferometry)	600	Vacuum standard items: EH	40
Experimental table	100	Electronics: Hardware and infrastructure (OH + EH)	800
Sample positioning (including gonio, hexapod and 2 piezo system, cameras)	230	Controls: PSS + EPS	120
KBs-Sample Interferometric control	100	Services	100
Forward direction area detector	2000	IT: Infrastructure - general (BL to CPD)	100
Area detector table (XYZ movements and rails)	120	IT hardware (within the BL)	100
Area detector on the robot	200	IT for data processing and on-the-fly data analysis (8 nodes with GPUs and 10 nodes with CPU) [a]	170
Diffraction robot including support	50	Data storage at the BL (disk based):285 k€/PByte, 3 PB/week before archiving [b]	855
Fluorescence detector (XRF)	100	Data archiving (tapes): 50 k€/PByte, 20 PB [c]	1000
XRF detector support (XYZ movements)	25	Software including licenses	50
HVAC experimental section (±0.2ºC)	200		

Estimated running costs: (a) 25 k€/yr. (b) 42 k€ x 3 PB/yr= 126 k€/yr. (c) 7.5 k€ x 20 PB/yr= 150k€/yr.

Total (k€): ***14770***
Contingency 15% (k€): ***2215.5***
Grand total (k€): ***16985.5***

6 – Based on main components (as defined in 3) provide simplified Gantt chart with key milestones and main dependences

Title	Duration	Start	End
1) Start project		1/1/24	1/1/24
2) Source	3y 4mo 2w	**1/1/24**	5/2/27
2.1) Design	4mo	1/1/24	19/4/24
2.2) Specs	4mo 2w	22/4/24	23/8/24
2.3) Tender	8mo	26/8/24	4/4/25
2.4) Production	2y	7/4/25	5/2/27
2.5) Delivery		5/2/27	5/2/27
3) Front End	3y 5mo	**1/4/24**	21/5/27
3.1) Design	4mo	1/4/24	19/7/24
3.2) Specs	5mo	22/7/24	6/12/24
3.3) Tender	8mo	9/12/24	18/7/25
3.4) Production	2y	21/7/25	21/5/27
3.5) Delivery		21/5/27	21/5/27
4) BLOptics	4y 4mo 2w	**22/7/24**	28/7/28
4.1) Design	1y 2mo 1w	22/7/24	22/8/25
4.2) Specs	6mo	25/8/25	6/2/26
4.3) Tender OptoMechanics	8mo	9/2/26	18/9/26
4.4) Production OptoMechanics	2y 1w	21/9/26	28/7/28
4.5) Delivery		28/7/28	28/7/28
5) Optical Hutch	2y 2mo	**25/8/25**	20/8/27
5.1) Design	9mo	25/8/25	1/5/26
5.2) Tender	8mo	4/5/26	11/12/26
5.3) Production	9mo	14/12/26	20/8/27
5.4) Delivery		20/8/27	20/8/27
6) Infrastructure OH	3y 2w 4d	**27/10/25**	17/8/28
6.1) Design+Procurement	1y	27/10/25	25/9/26
6.2) Infr. installation	1y 3w 4d	23/8/27	17/8/28
7) BL installation OH	2y 2mo 4d	**24/5/27**	24/5/29
7.1) ID+FE	6mo	24/5/27	5/11/27
7.2) Optics	10mo	18/8/28	24/5/29
8) Installation bridge pipe	8mo	11/9/28	20/4/29
9) Endstation	4y 10mo 2w	**3/3/25**	24/8/29
9.1) Design	2y 2mo 2w	3/3/25	12/3/27
9.2) Tender	8mo	15/3/27	22/10/27
9.3) Production	2y	25/10/27	24/8/29
9.4) Delivery		24/8/29	24/8/29
10) New Building Delivery		**30/4/29**	**30/4/29**
11) Infrastructure FEH	2y 6mo 1w	**24/5/27**	14/9/29
11.1) Design	1y 1w	24/5/27	28/4/28
11.2) Procurement	1y	1/5/28	30/3/29
11.3) Installation	5mo	30/4/29	14/9/29
12) BL installation FEH	6mo	**17/9/29**	1/3/30
12.1) Endstation installation	6mo	17/9/29	1/3/30
13) ALBA-II inst. shutdown	**1y 7mo 2w 1d**	**1/1/30**	**1/7/31**
14) Commissioning	3y 1mo 1d	**25/5/29**	26/3/32
14.1) OH Optics	7mo 2w 1d	25/5/29	21/12/29
14.2) Endstation w/o beam	1y 5mo 2w	4/3/30	4/7/31
14.3) Endstation w/beam	9mo 2w 3d	2/7/31	26/3/32

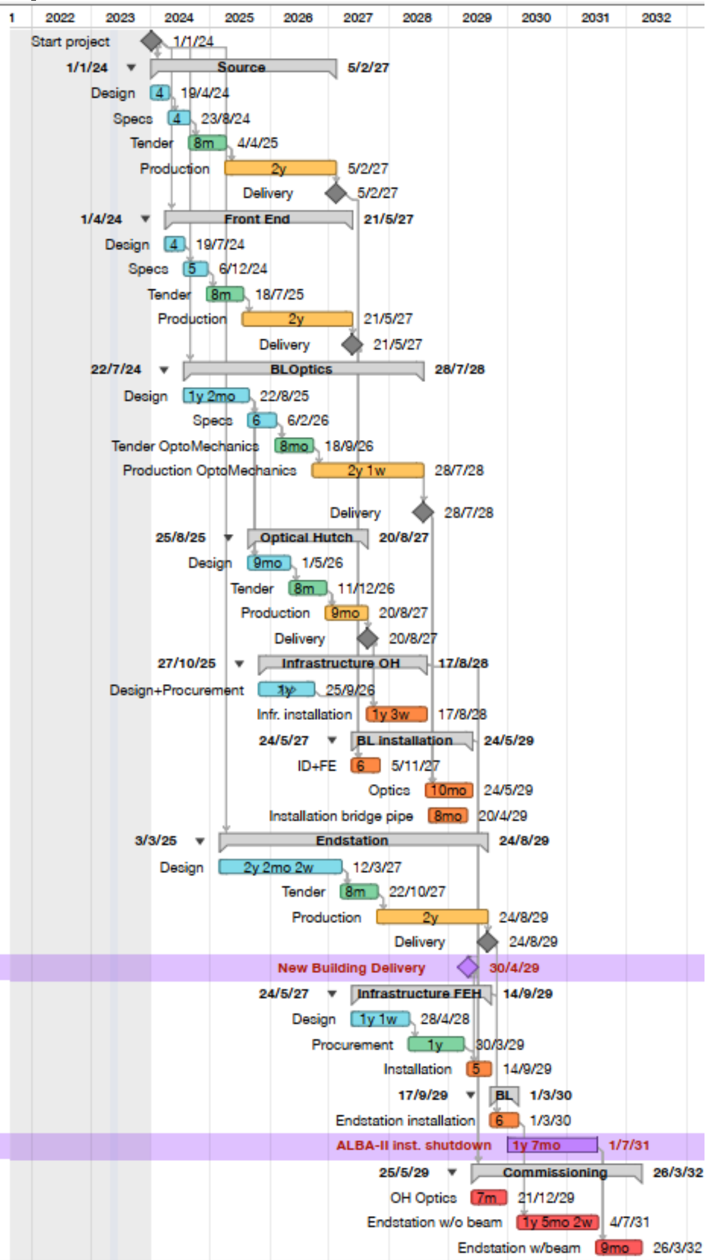

This planning has been defined following some guidelines and restrictions to minimize the mutual impact of the CoDI beamline construction, ALBA operation and ALBA II design and installation:

- It has been assumed a starting date of 01/01/2024, accommodating the resources for several years until ALBA II starts operation to ensure resource optimization. Also, some steps (*e.g.* end station design) has been extended to ensure that the latest technology will be implemented.
- The construction can be started within the ALBA experimental hall, independently of ALBA II, commissioning the beamline up to the secondary source.
- The installation of the far experimental hall (FEH) depends on the new building to be constructed, so the dates are tentative. This new building will contain the experimental hutch that will be made of barite concrete (not lead-based), so its installation is not included in the planning.

- ♦ The major installation has been programmed to finish before ALBA upgrade dark period (ALBA II installation) to release resources for accelerators and other beamlines. However, this depends on the availability of the new building and on the final start of the dark period, which are nowadays tentative dates.
- ♦ During ALBA II upgrade, commissioning without X-ray beam can be performed, including mechanics, controls system, and data analysis pipeline.

The CoDI beamline will provide different techniques based on a nano-focused beam. Therefore, an implementation plan has been defined depending on the complexity of the technique and the efforts required. The experimental implementation plan has been defined to initially commission the hardware and software, but also the X-ray beam properties (*e.g.* coherence of the source, the secondary source and the beam focus). Then, few techniques will be commissioned to be available for the users:

- nano-XRF and nano-diffraction during the commissioning of the nano-focus
- 2D Ptychography and holography
- Bragg-CDI

And after this first stage is completed obtaining the first good results, the second implementation phase will start to commissioning and releasing the following techniques:

- 3D coherent imaging
- Tele-ptychography
- Bragg-ptychography

Of course, CoDI will be an state-of-the-art beamline not only in hardware and X-ray beam properties, but also on the data analysis pipeline and creation of new methodologies, following the requirements and necessities of the scientific community to solve the societal challenges of the moment. This means that CoDI will always be updated with the last technology and methodology to serve the community.

7 – List of supporters

Dr. A. Rodriguez-Fernandez, Instrument scientist Eu XFEL, Germany (SP and PI)
Prof. P. Villanueva-Perez, Universidad de Lund, Sweden. (Co-PI)
Dr. A. Diaz, Beamline scientist Paul Scherrer Institute, Switzerland (SU and key advisor)
Dr. I. Calvo, Universidad de Zaragoza - INMA, Spain (SU)
Prof. M. A. G. Aranda, Universidad de Málaga, Spain (SU)
Dr. E. Solano, ALBA, Spain (SU)
Dr. L Aballe, ALBA, Spain (SU)
Dr. C. Popescu, ALBA, Spain (SU)
Dr. C. Huck Iriart, ALBA, Spain (SU)
Prof. J. Solla, Universidad de Alicante, Spain (SU)
Dr. V. A. de la Peña O'Shea, IMDEA Energy, Spain (SU)
Prof. A. Johnson, IMDEA nanociencia, Spain (SU)
Prof. J. A. Blanco, Universidad de Oviedo, Spain (SU)
Dr. C. Frontera, ICMAB, Spain (SU)
Prof. Dr. Javier Díaz, Universidad de Oviedo, Spain (SU)
Prof. J. A. Garrido, ICN2, Spain (SU)

The document should not exceed 40 pages